Chapter 1
Metallic Biomaterials

Robert M. Pilliar

1.1 Introduction – Why Metals?

Metallic biomaterials continue to be used extensively for the fabrication of surgical implants primarily for the same reason that led to their initial selection many decades ago. The high strength and resistance to fracture that this class of material can provide, assuming proper processing, gives reliable long-term implant performance in major load-bearing situations such as those experienced in certain orthopedic and dental implant applications. In addition, the good electrical conductivity of metals makes them a good material for making neuromuscular stimulation devices (e.g. cardiac pacers). These characteristics, coupled with relative ease of fabrication using well-established and widely available techniques (e.g. casting, forging, machining), as well as more recently developed manufacturing methods (i.e. additive manufacturing using selected laser melting or sintering) has promoted and continues to favor metal use in the fields of orthopedics, dentistry, and cardiovascular surgery, in particular. The favorable properties (good fracture resistance, electrical conductivity, formability) are related to the interatomic bonding and atomic arrangements that characterize metals. While the purpose of this chapter is to focus on the important issues pertaining to the processing and performance of metallic biomaterials and to review the metals that are currently used for implant fabrication, a brief review of fundamental issues related to the structure–property relations of metals, in general, follows.

Metal processing procedures determine metal microstructures that in turn determine material properties (elastic constants being an exception since these are structure-insensitive parameters dependent only on interatomic bond type and equilibrium atom packing as noted below) [1, 2]. An understanding of material properties and processes used to achieve these properties during fabrication of metallic

R. M. Pilliar (✉)
University of Toronto, Toronto, ON, Canada
e-mail: bob.pilliar@utoronto.ca

R. Narayan (ed.), *Biomedical Materials*,
https://doi.org/10.1007/978-3-030-49206-9_1

components is critical for achieving desired performance of implants. While mechanical failure is unacceptable for most engineered structures, it is particularly so for surgical implants where failure can result in patient pain, the need for complicated and life-threatening revision surgery and, in certain cases, death (e.g. heart valve component fracture).

1.2 Metallic Interatomic Bonding

Interatomic bonding in solids occurs by strong primary (ionic, covalent, and/or metallic) and weaker secondary interatomic bonding (van der Waals and hydrogen bonding). Metals are characterized by metallic interatomic bonding with valence shell electrons forming a "cloud" of electrons around individual atoms/ions. This is a consequence of the high coordination number, N, (i.e. number of nearest neighboring atoms) that characterize metals ($N = 12$ or 8 for many metals). As a result of this close positioning of neighboring atoms and the shared valence electrons, the interatomic bonds are nondirectional and electron movement within metal crystal lattices is easier than in ionic or covalently bonded materials. This fundamental distinguishing characteristic of metals results in the relative ease of plastic deformation (i.e. permanent deformation on loading above a yield stress) as well as the high electrical and thermal conductivities of metals. Most metals used for implant fabrication have either close-packed atomic structures with $N = 12$ with face-centered cubic (fcc) or hexagonal close-packed (hcp) unit cells, or nearly close-packed structures with $N = 8$ forming body-centered cubic (bcc) structures. Less commonly, tetragonal and orthorhombic as well as other unit cells do occur with some metallic biomaterials. The equilibrium distance between atoms defining the unit cells of these crystals and the strength of their interatomic bonding are determined by intrinsic factors such as atom size and valency as well as extrinsic factors (temperature, pressure). In addition to ease of deformation to desired shapes, the ability to deform plastically at high loads results in another very important feature namely the ability of most metals to blunt sharp discontinuities (through plastic deformation) thereby reducing local stress concentrations thereby resulting in relatively high fracture toughness that most metals display. As noted below, these desirable characteristics are dependent on proper selection of processing conditions during material and part preparation.

1.3 Crystal Structures – Atom Packing in Metals

The most common metallic biomaterials (i.e. stainless steel, Co-based alloys, and Ti and its alloys) form either face-centered cubic, hexagonal close-packed, or body-centered cubic unit cells at body temperature and during different stages of their thermal treatment with ideal crystal lattice structures such as those shown in

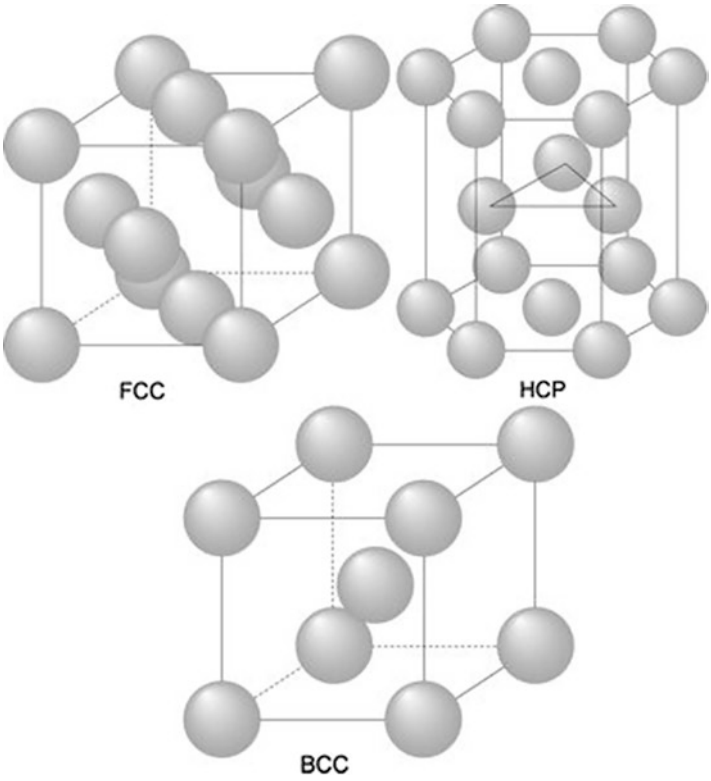

Fig. 1.1 Unit cells for face-centered cubic (fcc), hexagonal close-packed (HCP), and body-centered cubic (bcc) crystal structures. (Illustration courtesy of Dr Scott Ramsay, University of Toronto)

(Fig. 1.1). Real metal crystals, in contrast to these ideal atomic arrangements, contain lattice defects throughout (vacancies, dislocations, grain boundaries – Fig. 1.2). The presence of these defects (point, line, and planar defects) has a strong effect on mechanical, physical, and chemical properties.

Using a simple solid sphere model to represent atom packing, arrangement of spheres in the closest packed arrangement shown in Fig. 1.3. results in either a face-centered cubic structure (2-D planar layer stacking sequence as ABCABC… – Fig. 1.3a) or a hexagonal close-packed structure (ABABAB… stacking sequence – Fig. 1.3b). The selection of the preferred arrangement for a close-packed metal depends on the lowest free energy form under given extrinsic conditions (temperature and pressure). Regions of substitution of one stacking sequence for the other can occur locally and these represent another type of lattice defect (a stacking fault with its borders defined by partial dislocations [3]). While many metals used for implant applications form close-packed structures over a certain temperature range (e.g. Ti and its alloys are hcp below about 900 °C, Co-based alloys form fcc crystalline structures above approximately 850 °C, 316L stainless steel is fcc from its forging temperature ~ 1050 °C down to room temperature), others form less

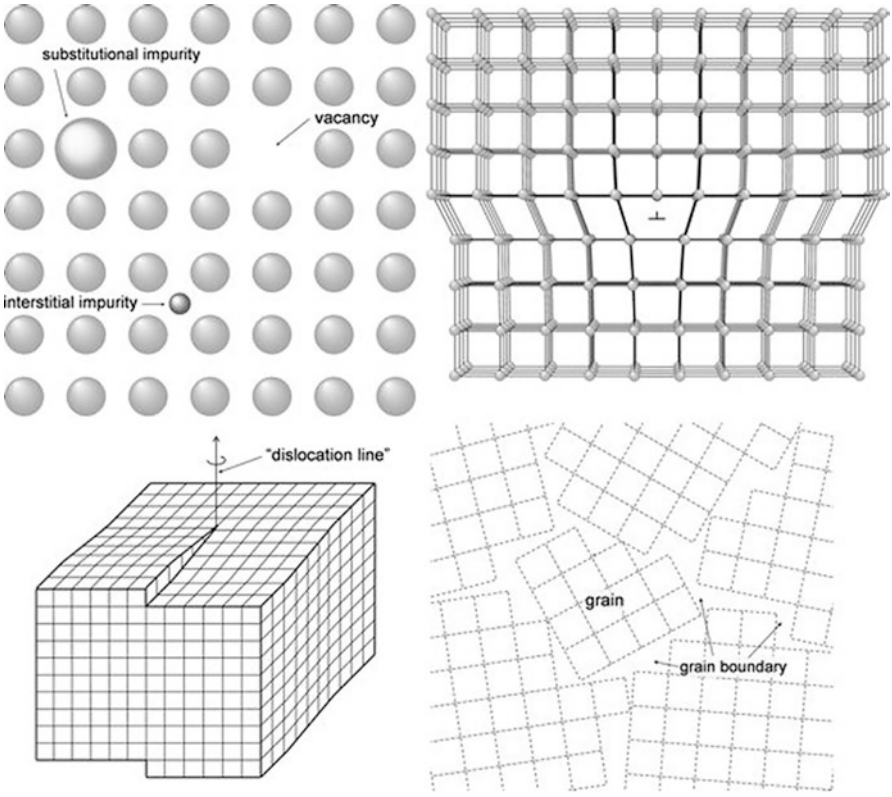

Fig. 1.2 Crystal structures showing point defects (substitutional or interstitial elements, vacancies), line defects (dislocations), planar defects (grain boundaries, twin boundaries)

closely packed structures (Ti and Ti-based alloys form bcc structures at elevated temperatures). Lowest free energy determines which crystallographic arrangement will exist under given conditions of temperature and pressure. Understanding the nature of the transformations that may occur during metal processing is important for achieving desired properties, but may also result in secondary phases with undesirable properties leading to unacceptable properties. A good understanding of constitutional (equilibrium) phase diagrams is important for the design of processing methods for forming metal implants. It should be appreciated, however, that these often, oversimplified equilibrium phase diagrams (i.e. limited to two- or three-element alloys rather than the multielemental compositions of most practical alloys) indicate, even for these simple compositions, equilibrium structures that may not be achieved during processing because of kinetic considerations as discussed below.

In view of current growing interest in nanocrystalline metals (crystal/grain size < 100 nm) in which grain boundary regions may represent a significant percent

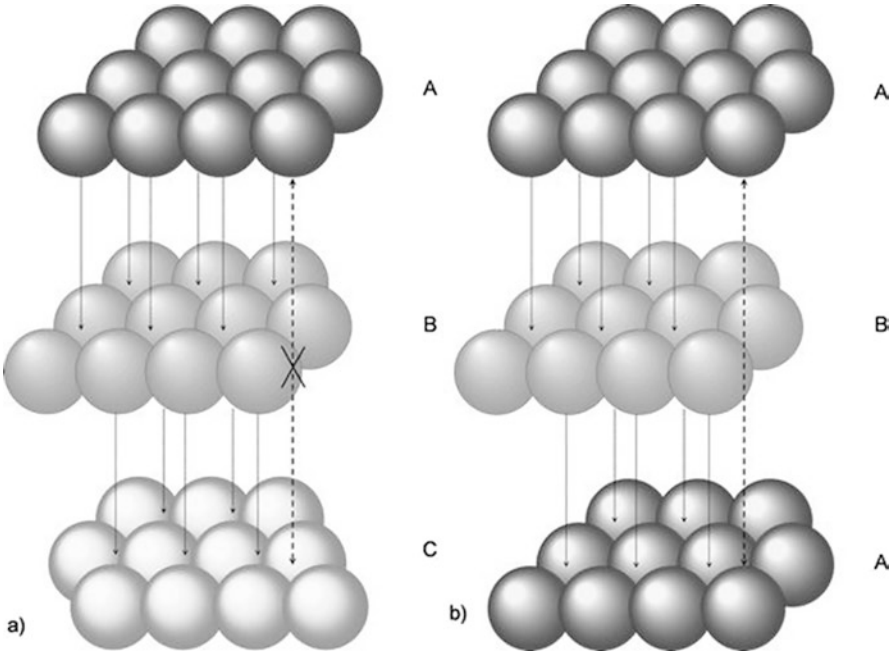

Fig. 1.3 Solid sphere models showing the two stacking sequences possible in close-packed crystal structures. The layering sequence of the close-packed planes is different, but the nearest number of neighboring atoms (coordination number) is 12 for both arrangements. (Illustration courtesy of Dr Scott Ramsay, University of Toronto)

of the overall material's volume and, as such, may significantly affect properties, it is important to understand grain boundary structures and properties. Grain boundaries are planar crystal defects in which atom disorder exists to a lesser or greater degree depending on the nature of the grain boundary [3]. The so-called low-angle grain boundaries with small orientation differences between adjacent grains can be represented by ordered arrangements of edge dislocations (described briefly below) creating the slight orientation differences while for large intergranular orientation differences, the boundary zones with higher dislocation densities give a highly disordered atomic arrangement approaching an amorphous state for some boundaries. Thus, grain boundaries, due to their atomic disorder, are high energy regions where reactions can preferably occur and higher atom diffusion rates can occur as well as deformation mechanisms not associated with dislocation movement and interaction. Grain boundary sliding even at low temperatures can explain observed plastic deformation.

1.4 Phase Transformations – Diffusive and Displacive

The equilibrium arrangement of atoms in solids is determined by factors such as atomic size, valence, and chemical affinity between elements under specific extrinsic conditions (i.e. temperature, pressure). For given temperature and pressure conditions, the stable state is the structure displaying lowest free energy. Free energy, G, is related to enthalpy, H, (heat of formation), and entropy, S, through the relation $G = H - TS$, where T is the absolute temperature. Changes in state or phase transformations in solids are possible if a decrease in G occurs due to the transformation (i.e. $\Delta G = \Delta H - T\Delta S < 0$ at the transformation temperature).

While a reduction in G represents a necessary thermodynamic condition for the formation of a new phase, atomic rearrangement to form the new phase must occur in a reasonable time period (a kinetic consideration). For most solid-state phase transformations, atom rearrangement occurs through thermally controlled diffusion processes (diffusive transformations) that result in both crystallographic and regional compositional changes within the newly formed phase(s), the amount and microstructure of the new phase(s) being dependent on temperature and time at temperature. Phase transformations can also occur through diffusionless processes that are not dependent on time at temperature but rather on temperature changes only or mechanical straining of samples at an appropriate temperature. These are referred to as displacive or *martensitic* transformations [4, 5]. They are *athermal*, meaning that the amount of new phase forming from a parent phase is dependent only on the final temperature (or degree of deformation at temperature). The transformation occurs very rapidly with the transforming wave-front sweeping across a sample at the speed of sound. Very small atom displacements are needed to achieve transformation. The temperature at which martensite first starts to form from the parent phase (austenite) is the M_s temperature (martensite start temperature) with 100% martensite forming at the M_f temperature (martensite finish temperature). Upon heating, the reverse transformation (martensite to austenite) starts at the austenite start (A_s) and finishes at the austenite finish (A_f) temperatures. There is hysteresis between the forward and reverse transformation processes reflecting the energy required for the transformation. Displacive transformations involve very slight repositioning of atoms within a crystalline solid in combination with a so-called *lattice invariant* strain that involves lattice *twinning* only to accommodate the overall shape change that would otherwise result from the cumulative small atom displacements. Some metallic biomaterials can transform through a displacive mechanism including CoCrMo and Ti-based alloys that are used extensively for joint replacement implants. The Ni-Ti shape memory alloys (SMA) are used currently in dental applications and are being investigated for implants in orthopedic and cardiovascular use. These also transform by a displacive transformation resulting in two related phenomena that are attracting considerable interest currently (i.e. the shape memory effect and superelasticity).

For Ni-Ti alloys, the net result of the austenite-to-martensite transformation is a highly twinned martensitic structure. The resulting twin boundaries are low energy

boundaries that are quite mobile. Thus, components can be readily deformed at lower temperatures (where the martensite phase is stable) resulting in a change in part shape. On annealing above the A_f temperature, the martensite is transformed back to austenite *with an accompanying reversion to the initial undeformed shape*. This is referred to as the shape memory effect and can be used to advantage in biomaterial applications to impart a mechanical force on tissue following implantation as the implanted device warms up to body temperature. This is described further in the section on *Ni-Ti Alloys.*

A second effect due to the martensitic transformation in Ni-Ti alloys is that of *superelasticity* (also referred to as *pseudoelasticity*). This effect results in a very low apparent elastic modulus for the Ni-Ti alloys. It is due to the formation of *stress-induced martensite (SIM)* during mechanical deformation of the austenite phase within a limited range of temperatures just above the A_s temperature and below a temperature defined as the M_d temperature, (the maximum temperature at which stress-induced martensite will form). Mechanical strain at this temperature provides the driving force for austenite-to-martensite transformation. However, the resulting stress-induced twinned structure forms with a preferred twin *variant*, a twin formed with a twin boundary defined by a specific crystallographic plane, (e.g. a (111) plane) in contrast to the formation of a family of twins having common boundary planes but differently oriented, for example having {111} boundary planes as occurs for the thermally driven shape memory transformation. The stress-induced transformation results in a significant overall elongation in contrast to the thermally driven one. The elongation is fully recovered on release of stress. The resulting stress-strain curve (Fig. 1.4) shows complete recovery upon unloading relatively large

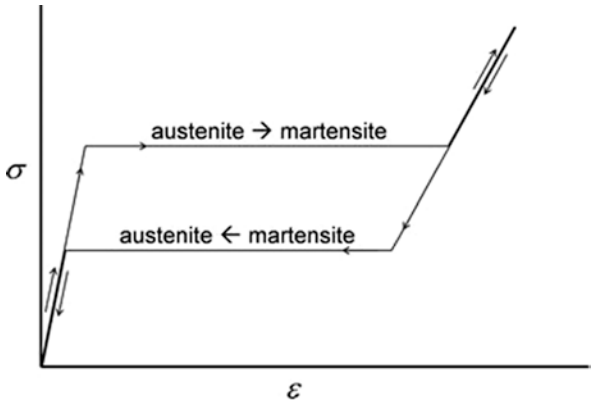

Fig. 1.4 Stress-strain curve for a metal (such as Ni-Ti alloy) displaying stress-induced martensitic transformation and superelastic behavior. Note the hysteresis on loading and unloading

strains (as high as 10% for some shape memory alloys) thereby resulting in a low apparent elastic modulus.

1.5 Diffusion in Metals

Atom diffusion occurs during metal processing and determines the structure and properties of metallic components. Hence, solidification during casting of a melt, grain growth during elevated temperature annealing of parts, the precipitation and growth of second phase particles, sintering of metal powders to form either dense or porous structures, bonding of films or coatings to substrates, recrystallization (in which relatively strain-free crystals nucleate and grow within mechanically deformed materials), and the formation of protective oxides over metal substrates (passive film growth) all involve atom diffusion. Thus, an understanding of atomic diffusion rates and mechanisms is important for design of processes for component formation with desired properties. The diffusion rate, D, is given by the equation $D = D_o \exp(-Q/RT)$ where D_o = diffusion coefficient (characteristic of an atom diffusing in a given material), Q = activation energy for atom movement, R = universal gas constant and T = absolute temperature. This relation shows that diffusion rates fall exponentially as temperature is reduced so that at some lower temperature, diffusion driven structural changes will not occur in practical time periods even though they are energetically favored by changes in free energy (i.e. $\Delta G < 0$). As a result, metastable structures can exist at ambient temperatures. The retention of an fcc-structured phase in Co-based alloys used for orthopedic implant fabrication is an example of this. The fcc structure (γ-phase) is metastable at temperatures below about 900 °C where free energy considerations would predict the formation of the hcp ε-phase. Slow diffusion of Co, Cr, and Mo atoms at and below the transformation temperature prevents the ready formation of the hcp phase by a diffusive transformation. The reaction is described as "sluggish" and, only under special circumstances, as discussed later, does the stable hcp phase form.

The formation of well-developed crystalline structures during solidification from the liquid state (or during other types of solid state formation reactions such as chemical or physical vapor deposition, processes that are being used for formation of films, coatings, and some porous structures) requires the movement of atoms to equilibrium lattice sites. Should very rapid cooling occur during solidification, such regular positioning of atoms is unable to occur and, instead, random atomic positioning and amorphous structures lacking long-range order will develop. Such amorphous structures occur more readily during solidification of complex ionically or covalently bonded nonmetals. These have relatively lower diffusion rates due to the large molecules that define the structures of these materials and the higher activation energies for molecule movement. Some metals can also form amorphous structures on solidification but only if very high cooling rates ($>10^6$ °C-s^{-1}) are used during solidification [6]. These display some interesting properties including high hardness and excellent corrosion resistance, characteristics that are desirable for

certain biomaterial applications. The high hardness can be explained by the fact that amorphous metals do not deform readily by dislocation glide as occurs with crystalline metals displaying simple lattice structures (see below). (The excellent corrosion resistance appears related to the fact that preferred, higher free energy sites for initiation of corrosion reactions such as grain boundaries and other lattice defects (vacancies) do not exist in these structures). These as well as nanocrystalline metals (grain size < 100 nm) that also display interesting properties such as excellent wear resistance, high strength, and corrosion resistance are discussed briefly in the *New Directions* section. These represent possible future developments for forming novel metallic implants or implant surface coatings.

1.6 Interatomic Forces and Elastic Moduli (*Structure-Insensitive* Properties)

All crystalline materials, as noted above, are formed with characteristic 3-D equilibrium atomic structures with specific atom arrangement/packing and equilibrium interatomic spacings that characterize that material. The interatomic forces acting on atoms in these equilibrium positions will be equal to zero as a result of a balance of attractive and repulsive force fields acting on the atoms (i.e. $F = dU/dr = 0$ where F = interatomic force, U = bond energy, a function of "r", and r = interatomic spacing – Fig. 1.5a, b). Small displacements from the equilibrium position in response to applied forces result in an increase in internal energy of the structure. The potential energy of an atom, U, can be described by an empirical equation of the form $U = -A/r^m + B/r^n$ where $m < n$ [1.1]. The first term of this equation is related to an attractive energy force (this force is lowered as atoms are brought closer together approaching the equilibrium spacing, r_o), while the second term is related to the repulsive force that develops as atoms are brought into too close proximity ($r < r_o$). The interatomic force-distance relation represents an intrinsic material characteristic relating small lattice deformations (atomic displacements) and the forces resisting these displacements. Stress and strain can be determined experimentally for a material with the initial slope of the stress vs. strain curve describing an intrinsic elastic constant for a material (Young's modulus, E, for very small tensile or compressive forces or Shear modulus, G, for shear forces). For small deformations in metals, the relation between stress and strain is linear and, except at higher temperatures approaching the melting temperature where atomic diffusion is rapid and creep deformation occurs, it is virtually strain-rate independent for metals. Assuming a regular 3-D cubic arrangement of atoms and an applied tensile force (one tending to increase the separation between atoms), a simple estimate of E can be made [1.2] giving Young's Modulus, $E = \sigma/\varepsilon = dF/r_o^2/dr/r_o = (1/r_o)\ (dF/dr)$ where σ = stress, ε = strain, F = interatomic force, r and r_o = interatomic and equilibrium interatomic spacing respectively. This suggests that E is directly related to the slope of the interatomic force-distance curve and inversely proportional to the equilibrium spacing

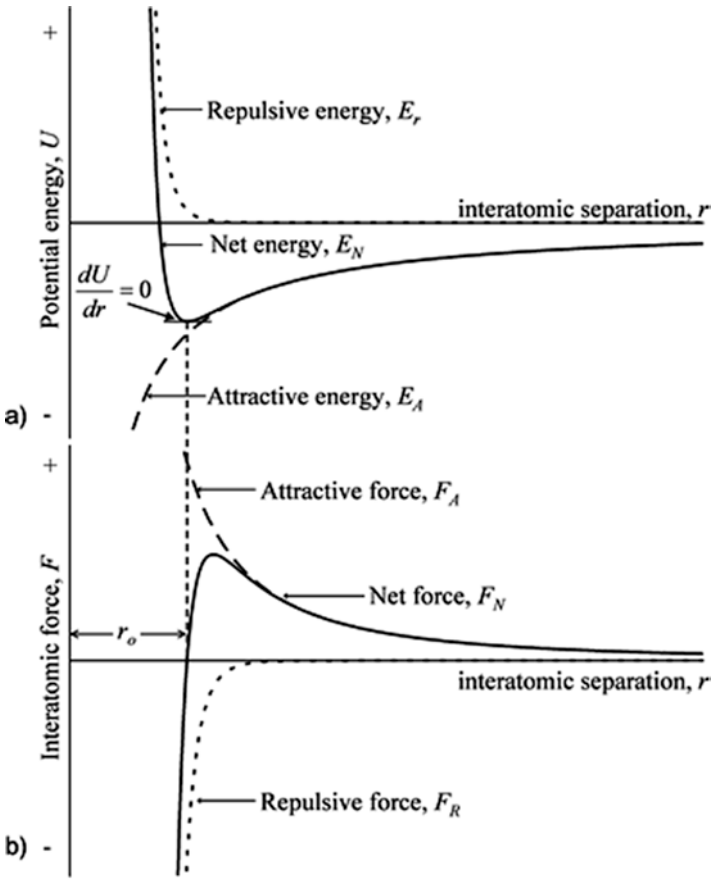

Fig. 1.5 Potential energy vs. interatomic separation curve (**a**) showing how the net effect of attractive and repulsive forces acting between atoms, as shown in (**b**), result in an potential energy minimum that defines the equilibrium interatomic separation

between atoms. Metal processing has very little influence on these two parameters so that elastic constants (E and G) can be considered intrinsic material properties independent of method of processing and the resulting microstructure (i.e. *structure-insensitive* properties). A third elastic constant, Poisson's ratio, υ, that describes the lateral deformation occurring as a result of axial elastic deformation ($\upsilon = -\varepsilon_y/\varepsilon_x$) for a force applied in the "x" direction) represents another *structure-insensitive* intrinsic material property. Table 1.1 summarizes some mechanical properties for a number of commonly used metallic biomaterials indicating a definite value for the elastic constants in contrast to the range of possible values for other mechanical properties. The range of these other properties is due to their dependence on material microstructure that, in turn, is a function of the method of processing used for material formation. Thus, in contrast to the elastic constants, these other properties are *structure-sensitive*. Also included in Table 1.1 are the elastic constants for some

Table 1.1 Mechanical properties of metallic biomaterials

Material	E (GPa)	σ_{yield} (MPa)	σ_{ult} (MPa)	% elong
Fe-based	200–205	170–690	540–1000	12–40
Co-based	220–230	450–1500	655–1900	5–30
CP Ti	100–115	170–480	240–550	15–24
Ti-based	100–110	585–1050	690–1150	10–15
Ta	188	140–345	205–480	1–30
Ni-Ti (Ms)	28–41	70–140	895	~9
Zr-2.5Nb	98	310–550	450–800	15–20
Mg-based	41–45	125–200	220–280	3–22
UHMWPE	0.5	–	~3	800
Al_2O3	350–380	–	400 (flexural)	–
PS-ZrO_2	200	–	800 (flexural)	–
Bone (cortical)	10–20	–	100–300	1–2

Small variations in E may be attributable to different measuring methods. The large range of strength and % elongation to failure properties are due to different material processing. Some polymer and ceramic, as well as cortical bone properties are shown for comparison

other biomaterials (polymers and ceramics) as well as bone (cortical and cancellous). The large difference in elastic constants for the metals commonly used for forming bone-interfacing implants for orthopedic applications (stainless steel, Co-based alloys, Ti and its alloys) and bone is noteworthy. This large disparity can lead to undesirable structural changes to bone situated next to a metallic implant in situations where the implants are (1) securely fastened to bone (a preferred situation for joint replacement and fracture stabilization) and (2) oriented with the length of the implant juxtaposing a significant length of bone (as for example a femoral hip implant stem component within the host femur). The effective composite construct comprised of bone and metal implant, in effect, is a reinforced composite so that major stresses are borne by the higher modulus metallic implant thereby "stress shielding" the host bone. Because of this, disuse atrophy and significant bone loss can result over time. In addition, abnormally high stresses can develop in bone at regions where force is transferred from the implant to the host bone (e.g. at the distal tip region of the femoral stem – Fig. 1.6). Studies to develop lower elastic modulus metallic alloys and/or lower stiffness implant designs to overcome this "stress shielding" effect represent an active area of current biomaterials research.

1.7 Plastic Deformation and *Structure-Sensitive* Properties

Metals display high degrees of ductility if appropriately processed, a direct consequence of the metallic interatomic bonding that allows relatively easy movement of crystal line defects (dislocations) along certain crystallographic planes (slip planes). Dislocations (edge and screw) are a type of crystal lattice defect (line defects) that occur within crystalline solids (Fig. 1.2). Their movement through the crystal lattice

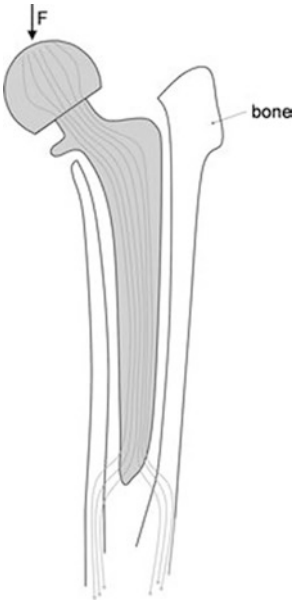

Fig. 1.6 Schematic illustration of a securely fixed metallic femoral hip implant component in the femur showing the direction and concentration of lines of force acting during loading. The stiffer implant component acts to shield the bone next to the proximal stem portion thereby promoting bone disuse atrophy (a stress shielding effect). Note also the concentration of forces resulting in stress concentration within bone at the distal stem region. (Illustration courtesy of Dr Scott Ramsay, University of Toronto)

allows plastic deformation or yielding of metals at force levels far below those predicted for shearing of crystal planes in idealized dislocation-free crystals. Plastic flow results in blunting of sharp geometric discontinuities that act as stress concentrators where crack initiation will occur. The force required to cause dislocation movement or "gliding" along a crystal plane is related to the strength of the interatomic bonding, since dislocation movement requires sequential breakage and reformation of interatomic bonds, as well as dislocation interactions with other lattice defects (other dislocations, grain boundaries, stacking faults, precipitates, vacancies, impurity, or alloying atoms). Significant dislocation movement and plastic deformation occur when stresses are above a material's yield stress (Fig. 1.7). To increase yield strength, a number of strategies can be used all aimed at increasing a metal's resistance to dislocation glide. These include *strain hardening* (also referred to as work hardening or cold working), alloying for substitutional or interstitial solid *solution strengthening*, *precipitation* or *second phase hardening*, and strengthening by *grain refinement*.

Strain hardening is achieved by mechanical working of a metal above its yield stress. It is a result of dislocations interacting with other dislocations during loading resulting in dislocation entanglements and pile-ups that inhibit further dislocation glide thereby resulting in higher forces for continued plastic deformation and, hence, higher yield stress. *Solid solution strengthening* occurs through addition of other elements to a pure metal (or through inadvertent impurity element contamination). This results in increased resistance to dislocation movement along slip planes. *Precipitation hardening or strengthening* is a result of the formation of second

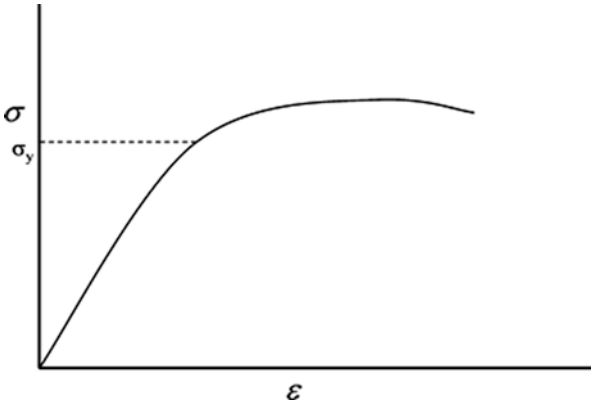

Fig. 1.7 Stress-strain curve for a metal showing the yield stress, σ_y. The yield stress is normally defined as the stress corresponding to either 0.1% or 0.2% plastic strain ($\sigma_{0.1\%}$ or $\sigma_{0.2\%}$)

phase precipitates that interfere with easy dislocation glide. (*Dispersion strengthening* is similar but usually refers to nonmetallic dispersoids within the metal matrix). G*rain boundaries* and *interphase boundaries* also inhibit dislocation movement since glide directions along preferred slip planes must change at such junctions. Finer grain size (and consequently more grain boundary area) results in higher yield strength as described by the Hall-Petch relation ($\sigma_y = \sigma_o + k/d^{1/2}$ where d = mean grain size and σ_o and k are empirically determined constants) [2]. This relation breaks down for metals with very small nano-sized or very large grains. All these possible strengthening mechanisms involve dislocation interactions with other dislocations or microstructural features that are determined by the processing routes for implant fabrication and that, in turn, determine the fate of implants during deployment and activation (e.g. vascular stents) and during functional repeated loading (e.g. orthopedic and dental implants, cardiac pacing leads). In addition to achieving sufficiently high yield strength to prevent unacceptable shape changes during functional loading, outright implant fracture must be avoided. Fracture can occur either as a result of a single overload event or through repeated (cyclic) loading at stresses well below the ultimate stress and even below the yield stress in the case of fatigue failure. Fatigue failure is a process resulting from the initiation and slow propagation of cracks during repeated loading of a part leading to its eventual catastrophic failure. This can occur in a relatively low number of cycles ($\leq 10^4$ cycles) (high repeated strains leading to low cycle fatigue, LCF) or over millions of cycles (low cyclic strain resulting in high cycle fatigue, HCF). For the former, relatively few loading cycles are required to initiate cracks so that crack propagation rates primarily determine fatigue strength. For HCF, the number of cycles for crack initiation can represent more than 95% of the total lifetime (measured in cycles to failure). Thus, its prevention is crucial for avoiding HCF failure. Fatigue crack initiation can occur at sites of dislocations interacting to create dislocation pileups leading to microvoid formation or where dislocation run-out at a free surface occurs creating surface stress risers (slip bands) promoting local crack initiation. Thus, processing to increase resistance to dislocation movement is a strategy for achieving higher yield strength and, hence, higher fatigue strength although yield strength increases

are accompanied by reduced ductility so that an optimal degree of strengthening will normally result in the highest fatigue strength. While fatigue fractures of contemporary orthopedic and dental implants are uncommon, they do occasionally occur and often after years of apparent satisfactory implant performance and millions of cycles of loading suggesting failure due to HCF conditions. This can be confirmed by examination of fracture surfaces using high resolution scanning electron microscopy (typically at magnifications > 1000 times). These studies often reveal the tell-tale signs of HCF, namely very finely spaced fatigue striations emanating from a fatigue crack initiation site (Fig. 1.8). In general, fatigue strength is related to yield strength so that the process used to achieve increased yield strength normally benefits fatigue strength. However, as noted above, strain hardening also results in decreased ductility which can lead to easier fatigue crack initiation so that careful selection of material processing procedures is necessary to achieve optimal static and dynamic (fatigue) properties of metallic components. Fracture toughness (K_c) or fracture energy (G_c) represents another important material property for consideration in device design. It is a measure of a material's damage tolerance characteristic. The ability of metals to deform plastically has a strong effect on fracture resistance since plastic deformation can result in blunting of sharp flaws thereby reducing local stress concentrations. This is the reason for the much higher fracture toughness values of metallic biomaterials compared to other high strength bioceramic materials such as Al_2O_3 or phase-stabilized ZrO_2 that are characterized by high compressive and much lower tensile strengths (see Table 1.2). Wear resistance is another necessary property of materials used to form articular bearing joint replacement components. Cast high-carbon CoCrMo alloys have been and continue to be used to form such components. High wear resistance is associated with high hardness, a characteristic that this alloy displays. This is due to the hard carbide

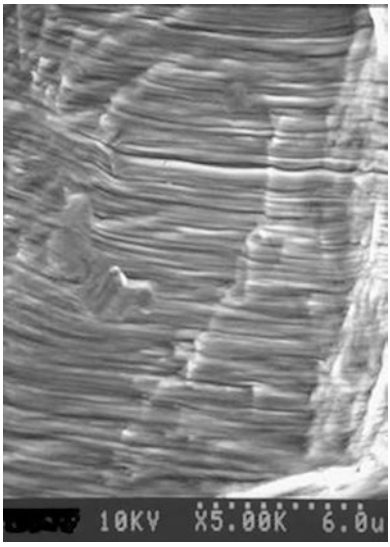

Fig. 1.8 Scanning electron micrograph of a CP Ti dental implant that had failed as a result of fatigue. The fatigue failure is clearly identified from the striations observed on the fracture surface. Note the high magnification needed to view the striations that have an approximate 0.5 μm spacing

Table 1.2 Metals used for orthopedic implant applications

Metal	Major/(minor) application	Processing route
Stainless steel	Osteosynthesis/(joint arthroplasty)	Hot/warm forming, machining
CoCrMo alloys	Joint arthroplasty/(osteosynthesis)	Casting, hot/warm forming, p/m
Co-Ni alloys	Osteosynthesis/(joint arthroplasty)	Hot/warm forming
CP Ti	Osteosynthesis	Hot/warm forming, machining
(α + β) Ti alloys	Joint arthroplasty & osteosynthesis	Hot/warm forming, machining
(β/near-β) Ti alloys	Osteosynthesis	Hot/warm forming, machining
Ni-Ti	Osteosynthesis	Hot/warm forming, machining
Ta	Bone augmentation	Chemical vapor infiltration
Zr-2.5Nb	Joint arthroplasty	Casting, machining

inclusions distributed throughout the alloy's microstructure, if appropriately processed, as well as its high work-hardening coefficient (i.e. high rate of work hardening during mechanical deformation, as would occur at the loaded bearing surface) [7]. There has been an increasing awareness in recent years of limits to the use of metal-on-metal (CoCrMo-CoCrMo) bearing joint replacements with evidence that excessive localized Co-alloy wear, largely due to edge wear of acetabular components, can occur. Associated with the resulting release of fine wear debris is the possibility of an allergic response resulting in what is referred to as an *adverse local tissue response*. This appears due to a high rate of Co and Cr ion release because of wear and corrosion of the fine wear debris and an allergic response to these ions in some patients. Resolution requires revision surgery and implant replacement (usually with an alternate material). A result of these unfortunate occurrences has been the reduction in metal-on-metal (i.e. CoCrMo-on-CoCrMo) implant use within the past decade or so. While other factors may contribute to failures, wear is recognized as an important contributor with wear resistance being an important requirement in joint replacement implant design. A related issue that is dealt with further in the next section (*Corrosion Resistance*) is the potential contribution leading to adverse local tissue response of metal ion release through fretting-corrosion at metal–metal junctions of modular implant designs. CoCrMo alloy-Ti6Al4V alloy junctions are common in such designs. Fretting, like wear, is due to mechanical breakdown of a material. The phenomenon can be exacerbated due to electrochemical corrosion (i.e. environmentally assisted fretting) thus indicating the need for consideration of material electrochemical stability as well as mechanical properties in implant design.

Yield strength, ultimate strength, ductility, fatigue strength, fracture toughness, hardness, wear, and fretting-corrosion resistance are examples of *structure-sensitive* properties that should be considered in selecting metal compositions for implant fabrication. Lattice defects or imperfections such as point defects (vacancies, interstitials) and planar defects (grain or crystal boundaries, twin boundaries, interphase boundaries) and the interaction of these with dislocations determine these *structure-sensitive* properties. How materials are processed determines the density of and interactions between these features and consequently the acceptable limits of use of components made from the materials.

1.8 Corrosion Resistance

Concerns over possible high rates of corrosion of biomaterials and the detrimental effect that this can have on biocompatibility represent the most important consideration in the selection of metallic biomaterials [8]. In fact, only relatively few metals are considered acceptable for surgical and dental implant fabrication (Table 1.1). This is based on their relatively low rates of corrosion if they are properly processed. Acceptable corrosion resistance for most of these relies on formation of well-adhered, dense, protective oxide surface layers (passive oxide films typically 5–10 nm thick) that are retained during in vivo use. Thus, Ti and its alloys, Ta, CoCrMo and Co-Ni alloys, Ti-Ni alloys, Zr-Nb alloys, and certain austenitic stainless steels rely on such passive oxide layers for in vivo corrosion protection. In addition, some metals made from more noble elements that do not rely on passive film formation and that display acceptable in vivo corrosion properties are used for some surgical implant and dental device applications. Pt and Pt-Ir are examples of metals used for fabricating neuromuscular stimulation electrodes, cardiac pacemakers being the most common example. Pt alloys are also used in vascular stents. Au alloys and Pd alloys are used for dental bridge construction and as components of dental crowns (porcelain-fused-to-metal crowns). These noble metals are able to resist corrosion to an acceptable degree even in the aggressive body/oral environment due to their inherent chemical stability. Those metals that rely on passive oxide film protection, in contrast, are extremely reactive in oxygen-containing environments. This characteristic is used to advantage, for forming, and re-forming (should the passive oxide layer be breached) the well-adhering, dense oxide layers that develop either spontaneously during use or through chemical (immersion in nitric acid solution, for example), electrochemical (anodic film formation), or thermal (air oxidation) treatment as the final step in manufacture of implants from these metals. The important characteristic of these passive oxide layers is their relative stability in vivo, providing effective barriers to electron and ion transport. And while film growth and ion release can continue in vivo, the rate is sufficiently low to allow the safe use of these alloys. A concern arises, however, when very fine nano-sized particles are formed, for example, as a result of wear. The passive oxide films can be mechanically disrupted resulting in metal ion release until re-passivation of a breached protective film occurs. Fretting corrosion is an important issue that needs to be considered in material selection and modular implants used in orthopedics. The development and use of coatings or other forms of implant surface modification for added protection represent ongoing studies with the goal of improving implant performance. The latter is a strategy being explored in developing novel Mg-based biodegradable alloys for which unacceptably high corrosion/degradation rates is a major challenge.

1.9 Metals and Processes for Implant Fabrication

As already noted, only a relatively small number of metals are used currently for making surgical implants, primarily because of concerns over metal corrosion and biocompatibility. The metals used for making orthopedic implants either for use in reconstructive surgery (joint replacement and skeletal augment implants) and trauma treatment (fracture repair) or in spinal fusion procedures are listed in Table 1.2. These represent metallic biomaterials used in major load-bearing applications that can provide sufficient corrosion resistance, strength, and fracture resistance for long-term function (joint replacements) or shorter-term use (fracture fixation). Mg alloys that are designed to be biodegradable, in contrast, are designed to corrode but at an acceptable rate. Implant loading conditions can be complex and occur in an aggressive body environment so that good corrosion-fatigue resistance is a major property requirement. (Corrosion-fatigue describes the added effect of a corrosive environment on fatigue crack initiation and propagation). Joint replacement implants must also display good wear resistance since wear debris generated at articulating joint surfaces and as debris due to fretting at material contact junctions can either of itself or following degradation through corrosion result in unacceptable host reactions leading to implant loosening and other unacceptable consequences (e.g. *adverse local tissue response)*. Ideally, joint replacement prostheses should function reliably for decades. Unfortunately, even with today's biomaterials and implant designs, this is not always the case. For implants used in fracture repair and other osteosynthesis procedures (e.g. osteotomy healing), the requirements are less stringent since these devices usually can be removed following bone healing (i.e. after months or so), although this is not always done in practice.

The commonly used metals and some newer alloys that are being investigated currently are reviewed below. Further information can be found in other review articles on this subject [9, 10]. The focus of the present chapter is on the processing of metallic biomaterials and how processing determines properties, particularly fatigue strength, wear, and corrosion resistance, important parameters influencing implant success. The basic mechanisms outlined above are used to rationalize the process–property relations and selection of methods for implant manufacture.

1.9.1 Austenitic Stainless Steel (ASTM F 138/139, F 1314, F 1586, F 2229)

The stainless steel compositions (all fcc austenitic stainless steels) recommended for implant use are listed in Tables 1.3a, 1.3b, 1.4a, and 1.4b. Further information on stainless steels used in medical applications can be found elsewhere [11].

316L austenitic stainless steel (ASTM F 138/139), despite its greater susceptibility to crevice corrosion compared to other common metallic biomaterials, has over

Table 1.3a Compositions (in wt%) of austenitic stainless steels used for orthopedic implant fabrication

ASTM#	C	Mn	P	S	Si	Cr	Ni	Mo	N	Cu	Other
F 138	0.03	2.0	0.025	0.01	0.75	17.0–19.0	13.0–15.0	2.25–3.00	0.10	0.50	
F 1314	0.03	4.0–6.0	0.025	0.01	0.75	20.5–23.5	11.5–13.5	2.00–3.00	0.20–0.40	0.50	0.1–0.3 Nb 0.1–0.3 V
F 1586	0.08	2–4.25	0.025	0.01	0.75	19.5–22.0	9.0–11.0	2.00–3.00	0.25–0.50	0.25	0.25–0.8 Nb
F 2229	0.08	21–24	0.03	0.01	0.75	19.0–23.0	0.10	0.50–1.50	0.90 (min)	0.25	

Ref– Handbook of Materials & Med Devices – ed. JR Davis, ASM 2003

Table 1.3b Mechanical properties of austenitic stainless steels used for orthopedic implant fabrication; higher and lower values correspond to cold-worked and fully annealed samples, respectively

ASTM #	σ_{yield} (MPa)	σ_{ult} (MPa)	% elong	$\sigma_{fatigue}$ (10^7)
F 138	190–690	490–1350	<12–40	190–700
F 1314	380–860	690–1035	12–35	–
F 1586	430–1000	740–1100	10–35	–
F 2229	590–1550	930–1730	12–50	–

Ref– Handbook of Materials & Med Devices – ed. JR Davis, ASM 2003

Table 1.4a Compositions (in wt%) of CoCrMo and Co-Ni alloys used for orthopedic implant fabrication

ASTM #	Cr	Mo	Ni	Fe	C	Si	Mn	W	P	S	Other
F 75	27–30	5–7	1.0	0.75	0.35 max	1.0	1.0	0.2	0.02	0.01	0.25 N; 0.3 Al; 0.01 B
F 799 (low-C)	26–30	5–7	1.0	0.75	0.05	1.0	1.0	–	–	–	0.25 N
F 799 (high-C)	26–30	5–7	1.0	0.75	0.25	1.0	1.0	–	–	–	0.25 N
F 563	18–22	3–4	15–25	4–6	0.05	0.5	1.0	3–4	–	0.01	0.50–3.50 Ti
F 562 (MP35N)	19–21	9–10.5	33–37	1.0	0.025 max	0.15	0.15	–	0.015	0.01	1.0 Ti
F 90	19–21	–	9–11	3.0	0.05–0.15	0.40	1.0–2.0	14–16	0.04	0.03	–
F 1058 (Elgiloy)	19–21	6–8	14–16	Bal	0.15	1.2	1.0–2.0	–	0.015	0.015	0.10 Be; 39.0–41.0 Co

Ref– Handbook of Materials & Med Devices – ed. JR Davis, ASM 2003

Table 1.4b Mechanical properties of CoCr and Co-Ni alloys after different treatments

Process description	σ_{yield} (MPa)	σ_{ult} (MPa)	% elong	$\sigma_{fatigue}$ (10^7)
CoCrMo alloys				
F 75 – Cast + Solution annealed	450–530	655–890	11–17	207–310
F 75 – Cast + Porous-Coated	~490	~735	~11	150–207
F 799 – Forged (Low C)	875–995	1320–1450	19–26	670–800
F 799 – Forged (Low C) + P-C	~410	~815	~33	–
F 799 – Forged (High C)	~1175	~1510	~10	–
F 799 – Forged (High C) + P-C	600–840	1030–1280	~18	~240
P/M D-S (As-forged)	840	1280	–	690–895
P/M D-S + P-C	–	–	–	345
Co-Ni alloy (MP35N) – F 562				
Annealed (1050 °C)	300	800	40	340
Cold-worked (50% Red in Area)	650	1000	20	435
Cold-worked + aged	1900	2050	10	405
Other Co alloys				
F 1058 c-w + aged (wire)	1240–1450	1860–2275	–	–
F 563 c-w + aged	827–1172	1000–1310	12–18	–

decades been and continues to be widely used for making fracture repair devices mainly because of its low cost and ease of fabrication. It is also used for making joint replacement components in some regions where economic considerations so dictate. Stainless steel is also used for making vascular stents. The corrosion resistance of stainless steel is dependent on the formation of a thin Cr(+Mo)-containing passive surface oxide layer, the Mo imparting stability to the oxide in a Cl^--containing environment such as occurs in vivo. It exists as a single-phase alloy (fcc austenite phase) from its forging temperature (~1050 °C) to room temperature and achieves its reasonable strength and fatigue resistance through strain hardening and solid solution strengthening mechanisms and a fine grain size. Typically, implants are forged or otherwise hot-worked (e.g. rolling or extruding) at temperatures starting at 1050 °C and continuing through a series of working and re-annealing steps until a desired final shape is achieved. Working at the elevated temperature facilitates shaping since dislocation entanglements and pile-ups that would result in strain hardening at lower temperatures are eliminated. This is a result of microstructural *recovery* and *recrystallization*, processes that occur during the elevated temperature mechanical working. *Recovery* involves dislocation rearrangement to form lower energy dislocation networks, (*polygonization* and sub-grain formation) and *recrystallization* is a process by which new strain-free crystals nucleate within a mechanically worked microstructure. Thus, easy plastic deformation and shaping without the danger of component cracking is possible using elevated temperature processing. As parts cool during working, they eventually reach the recrystallization temperature, (the temperature needed to cause nucleation of strain-free crystals ~1000 °C for stainless steel), so that continued working below this temperature results in strain hardening of the alloy. This lower temperature "finish forming" is

useful for achieving a desired yield strength for a final component. The final properties (yield, ultimate strength, ductility, and most importantly, fatigue strength) are dependent on the degree of "cold" working that is imparted during this lower temperature mechanical deformation. Achieving a fine, uniform grain size is also important (for 316L an ASTM No. 5 grain size is recommended; i.e. ~ 60–65 μm cross-sectional dimension). Higher nitrogen content in some stainless steels (ASTM F 1314, ASTM F 1586, ASTM F 2229) results in higher strength (due to greater solid solution strengthening) as well as improved crevice and pitting corrosion resistance. The latter composition (ASTM F 2229) is a Ni-free, nitrogen-strengthened austenitic stainless steel with a higher Mn content (an fcc stabilizing element like Ni) resulting in the retention of fcc austenite despite the lack of austenite-stabilizing Ni. As with the original 316L stainless steel, the corrosion resistance of all these alloys depends on the formation of a passive Cr(+Mo) oxide layer. While all these austenitic stainless steels are nominally single-phase fcc alloys, carbides can form within the structure due to the small amount of C in these alloys if they are exposed to temperatures in the 400–800 °C range for significant periods. In this range, $M_{23}C_6$ phases can form at grain boundaries (M being Cr primarily) with associated depletion of Cr from adjacent zones. The resulting denudation of Cr from those regions results in a structure that is more susceptible to intergranular corrosion because of the resulting less stable passive oxide film next to the grain boundary region. This is referred to as alloy "sensitization" and to minimize the possibility of its occurrence, low carbon levels are recommended for load-bearing austenitic stainless steels (hence the "L" in 316L with $C = 0.03$ wt% maximum). An additional requirement for forming these steels is the use of vacuum melting during solidification. This ensures that nonmetallic inclusion levels can be kept to a minimum. Such inclusions, if present, would act as stress concentrators thereby reducing mechanical properties (particularly fatigue strength) of components as well as making component fabrication to final shape more difficult. Following final shaping of forged implants, they are ground and polished to a desired surface finish and then subjected to a "passivation treatment" using a recommended procedure (e.g. exposure to a 40% HNO_3 solution or thermal oxidation treatment – ASTM F 86). Other grades of stainless steel are used in other surgical implant applications [9, 10]. These include austenitic stainless steels such as types 304 and 316 (C levels up to 0.08 for the latter as opposed to 0.03 maximum for 316L) in wire form for surgical sutures (316L is also used for this application). Austenitic stainless steels are also used for fabricating vascular stents as well as electrodes, conducting lead wires and pulse generator housings of cardiac pacing systems (304, 316, 316L alloys). The fabrication of vascular stents presents a particular challenge since these devices experience extensive change in shape during expansion to their "working" diameter in vivo. To attain this characteristic, intricate designs that allow this while keeping local strains in the metal within safe limits thereby avoiding the danger of extensive yielding and fracture are used. One method for forming such intricately designed forms is by laser machining fine patterns into thin-walled cylindrical tubes with highly polished surfaces [12].

Precipitation-hardenable stainless steels are very high strength stainless steels used for making neurosurgical aneurysm and microvascular clips, applications requiring high yield strength characteristics. The alloys used are classified as semi-austenitic (e.g. 17-7PH) and martensitic (e.g. 17-4PH) stainless steel with the former (semi-austentic) being heat treated to transform it from its fcc solution-annealed state to a martensitic form. Subsequent hardening anneals of both classes result in the formation of precipitates throughout their microstructures giving further hardening and the desired high strength products. Corrosion resistance is lower than that of austenitic stainless steels but sufficient for the intended applications. Ferritic stainless steels (Series 400 stainless steels – bcc crystal structures) are used for making various surgical and dental instruments. They are transformed by heat treatment to form high strength martensitic structures. Some Series 300 stainless steels (fcc structures) are also used for fabricating non-implantable devices with the degree of cold working determining the final strength and fracture resistance of the products.

1.9.2 Co-Based Alloys

Co-based alloy implants for orthopedic applications can be formed by casting or forging, the latter using bar or rod stock made by conventional forming of cast billets (rolling, extrusion), or by hot isostatic pressing of Co alloy powders [13]. Additionally, a novel method for near net-shape formation of parts from metal powders (metal injection molding or MIM [14]) has been reported. CoCrMo implant alloys all contain Cr (~ 26–30 wt %), Mo (5–7 wt%), some Ni (1 wt% maximum in order to minimize concerns related to possible Ni sensitivity), other residual trace elements (Mn, Fe, Si, N), and C (either low-C ~ 0.05 wt% or high-C ~ 0.25 wt%) (Table 1.5).

1.9.2.1 Cast CoCrMo (ASTM F 75)

CoCrMo alloys for orthopedic applications, (primarily joint replacements), cast to near final form (high-C) are made by investment casting (lost wax process). This involves the simultaneous casting of a number of components onto a so-called casting tree from which individual parts are cut, ground, honed or otherwise treated to achieve the final implant form and surface characteristics including highly polished

Table 1.5 Interstitial element limits and mechanical properties for CP Ti (Grades 1–4)

Grade	O (max)	N (max)	H (max)	σ_{yield} (MPa)	σult (MPa)	% elong
1	0.18	0.03	0.015	170	240	24
2	0.25	0.03	0.015	275	345	20
3	0.35	0.05	0.015	380	450	18
4	0.40	0.05	0.015	483	550	15

surfaces of regions forming articulating bearing surfaces. The high-C alloys represent the most wear resistant metallic biomaterials currently available commercially, a result of the $M_{23}C_6$ (mainly), M_7C_3, and M_6C carbides (where M is primarily Cr) that form throughout their structure during solidification (Fig. 1.9a). The alloy, after solution treatment (see below) displays a high rate of work hardening [7] that may also contribute to this good wear resistance through hardening of the surrounding Co-based matrix upon application of bearing forces during functional loading. Alloy melting occurs between 1350 and 1450 °C depending on the exact composition of the alloy and forms a typical as-cast, cored structure on solidification with the major phase being face-centered cubic (fcc) (austenite designated as either γ- or α-phase in the literature) and the interdendritic zones being enriched in Cr, Mo, and C. The γ-phase forms at temperatures above 890 °C while a hexagonal close-packed (hcp) structure is stable below this temperature. However, because of the sluggish nature of the fcc to hcp transformation, a metastable fcc phase is normally retained to room temperature. Subsequent aging at below 890 °C or extensive mechanical deformation at the lower temperature results in the formation of either *faulted* fcc zones (*stacking faults* or regions where the ABCBABC stacking sequence to form

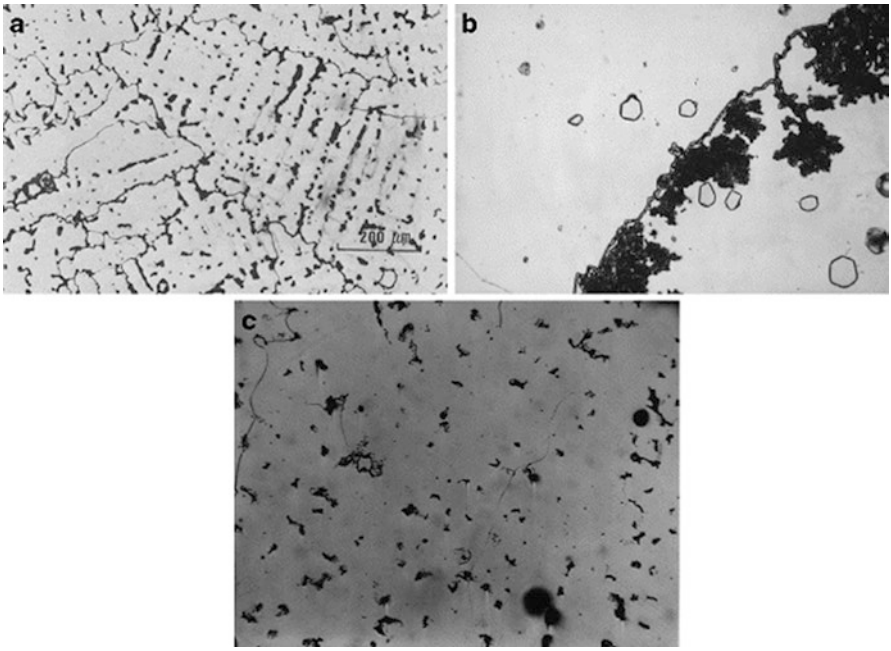

Fig. 1.9 Scanning electron micrographs showing microstructures of (**a**) a polished sample of as-cast high carbon CoCrMo alloy; note the relatively large grains, the heterogeneous composition evident from the different response to chemical etching used to show the microstructure; the darkest regions correspond to carbides dispersed throughout; (**b**) discontinuous $M_{23}C_6$ forming from γ-phase grain boundary region; (**c**) solution-annealed CoCrMo alloy (**c**) showing more homogeneous structure but with some retained carbides throughout

an fcc structure is altered to ABABAB stacking forming hcp zones with associated partial dislocation boundaries within the fcc phase) or hcp bands (formed by a displacive (martensitic) phase transformation mechanism). Aging between 650 and 850 °C favors $M_{23}C_6$ precipitation in the hcp zones but while this does increase yield strength, it also reduces ductility to unacceptable levels making such an aging treatment impractical [15]. As already noted, during solidification, a highly cored structure develops with interdendritic Cr-, Mo- and C-rich regions that can form extensive carbide networks and other brittle intermetallic phases (σ-phase) resulting in low ductility. (Figure 1.10 represents a pseudobinary phase diagram that predicts the formation of the heterogeneous, cored structure during normal cooling). To partially homogenize the structure, the as-cast alloy is treated with a short (~ 1 h) solution anneal at between 1200 and 1225 °C (below 1235 °C since this corresponds to a eutectic melting temperature for the Cr-, Mo-, C-enriched interdendritic regions and heating above this temperature would result in melting of the these zones [16] Fig. 1.10). Following the solution anneal, the alloy is cooled rapidly through the 1100–800 °C temperature range to avoid precipitation of embrittling $M_{23}C_6$ carbide networks. These can form as discontinuous carbide precipitates nucleated at and growing out from the γ-phase grain boundaries if sufficient time is allowed (Fig. 1.9b). The 1 h solution anneal treatment results in only partial homogenization of the cored structure but sufficient to give acceptable ductility (11–17% elongation). Some carbide dissolution does occur but enough of the hard carbide regions are retained to provide desired wear resistance (Fig. 1.9c). The major limitation of

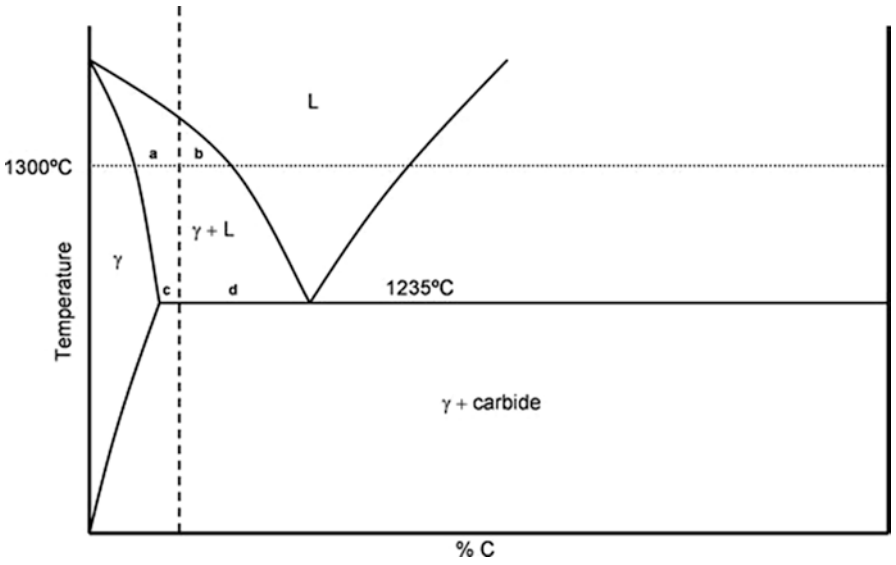

Fig. 1.10 Pseudobinary phase diagram showing a eutectic point at 1235 °C. The *vertical dashed line* corresponds to an alloy with a C content that on sintering at 1300 °C and rapid cooling would result in a:b relative ratio of carbide to γ-phase. Slow cooling from 1300 °C to below the eutectic temperature would result in a lower relative amount of carbide (i.e. carbide:γ-phase ratio = c:d)

Table 1.6 Mechanical properties of Ti alloys

Alloy	E (GPa)	σ_{yield} (MPa)	σ_{ult} (MPa)	% elong	$\sigma_{fatigue}$ (10^7)
α-β alloys					
Ti-6Al-4V	110	860	930	10–15	610–625
Ti-6Al-7Nb	105	795	860	10	500–600
Ti-5Al-2.5Fe	110	820	900	6	580
β/near-β alloys					
Ti-12M0-6Zr-2Fe (TMZF)	74–85	1000–1060	1060–1100	18–22	525
Ti-15M0-2.8Nb-0.2Si-0.26 (21SRx)	83	945–987	980–1000	16–18	490
Ti-35.5Nb-7.3Zr-5.7Ta (TNZT)	55–66	793	827	20	265
Ti-13Nb-13Zr	79–84	863–908	973–1037	10–16	500

the cast and solution annealed CoCrMo alloy is its relatively low mechanical properties (other than wear resistance) (Table 1.6). This is due to the coarse grain structure (> hundreds of microns and up to mm in size), inherent casting defects and shrinkage porosity resulting upon solidification and relatively slow cooling of the castings. In addition, the carbides that are retained after the solution anneal, while beneficial for wear resistance, create easy crack propagation pathways. Internal porosity (shrinkage pores) can be eliminated by hot isostatic pressing (HIP), thereby improving properties. HIP treatment has been reported to successfully improve poor quality castings but, not surprisingly, it does not significantly benefit already sound castings. However, this process does not heal surface connected defects so these can still act as preferred sites for early crack initiation. Corrosion resistance, as with the stainless steels, is dependent on the formation of a passive Cr- and Mo-containing oxide. This passive oxide layer is normally formed by nitric acid solution treatment as a final step in implant manufacture (ASTM F 86).

1.9.2.2 Wrought CoCrMo (Low- and High-Carbon) (ASTM F 799, F 1537)

Warm or hot forging of cast CoCrMo billets can result in significantly higher mechanical properties. Such thermomechanical treatment was used initially only with low C-containing alloys (C ~ 0.05 wt %). The lower carbon content resulted in fewer and smaller carbides throughout the structure thereby improving the alloy's formability but at the cost of reducing wear resistance. For hot forging, billets are heated to temperatures between 1000 and 1150 °C. Re-annealing at stages during the forging process is used in order to prevent edge cracking during deformation. Final implant shapes can be achieved using closed-die forging and a series of forging and re-annealing steps. A lower temperature finish forging operation, as with the stainless steel alloys, is used to achieve a degree of strain hardening of the alloy and a final form with desirable mechanical properties. Yield, ultimate and fatigue strengths are significantly higher than for the high-C, cast alloy despite the lower carbide content. This is a result of the much finer grain size, possible stacking fault

or hcp band formation, and strain hardening due to the lower temperature working operation all of which contribute to increased resistance to dislocation gliding and, hence, higher yield and fatigue strength (Table 1.5). As noted in Table 1.6, the fatigue endurance limit for hot-forged, low-C CoCrMo alloy is greater than 600 MPa. The wear resistance of the low-C alloys is poor compared with the higher-C cast alloy thereby negating their use for femoral ball or other surface bearing components.

Closed-die forging of high-C CoCrMo alloys is also possible although the procedures for so doing are difficult and very close control on forging and re-annealing stages is necessary. The result is a fine-grained and strain-hardened alloy with the additional benefit of the break-up of the larger carbides formed during solidification. This gives a high strength alloy with good wear resistance as a result of the finely distributed carbides throughout the structure. Whether cast or high-C wrought Co-based alloys provide superior wear resistance remains controversial. The fine carbide distribution does allow improved surface finishing of components and this may contribute to better wear behavior although supporting evidence based on long term clinical comparisons has not been presented.

Fine-grained, high-C bar stock that is suitable for subsequent closed-die forging to final shape can also be formed using a *powder metallurgy* processing route. By this method, high carbon CoCrMo alloy powders are formed by atomization (either by inert gas atomization or by a rotating electrode process [10]). The powders so formed represent very rapidly solidified "micro-castings" so that while retaining carbides and a cored structure (like the cast alloy), these are small and finely distributed (Fig. 1.11). After atomization, the powders are sized by screening and then consolidated to full density by placement in a suitable containment vessel that is evacuated, sealed and hot isostatically pressed (at around 1100 °C for 1 h at 105 MPa pressure) or hot forged, to form full density CoCrMo alloy. During the period at elevated temperature, some grain coarsening occurs but it is limited in extent because of the grain growth inhibition effect of the finely distributed carbides. A dispersion strengthened powder-made alloy formed by adding La and Al to the melt stock prior to atomization resulting in finely dispersed La and Al oxide particles

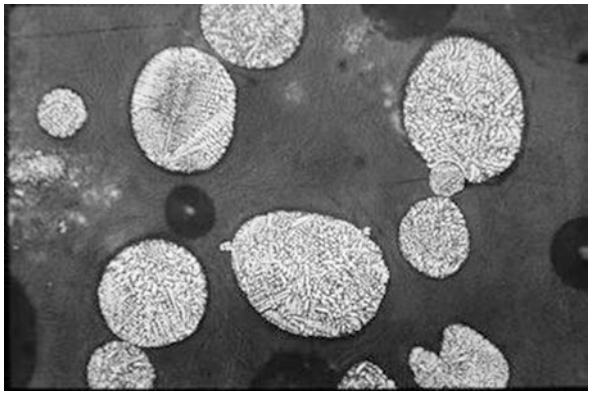

Fig. 1.11 Scanning electron micrograph of ground and polished atomized CoCrMo powder showing the fine cored microstructure within the powder a result of the relatively rapid cooling rate during atomization

throughout the HIPed alloy has been reported [17]. The rationale for introducing these finely dispersed oxides in this case is to inhibit grain growth during a subsequent high temperature sinter anneal treatment that is used for forming a sintered porous surface coating on the implants; this process is described below. The containment vessel outer layer is subsequently removed yielding a fine-grained CoCrMo alloy containing finely distributed carbides. The fine microstructure of the resulting bar allows easier hot or warm forging to a near final form (compared with coarser-structured alloys). Implants of relatively high strength, with good honing and polishing characteristics and good wear resistance can be formed using this metal powder-formed material.

Other novel methods such as metal injection molding (MIM) are being investigated for forming near final shapes from CoCrMo alloy powders [14]. The process involves mixing fine atomized powders with an organic binder, and extruding the resulting slurry to form pellets. These are then treated to remove the binder using a solvent and thermal decomposition during heating to the final sintering temperature that is just below the alloy's melting temperature (1340–1380 °C). (It is likely that some liquid phase contributes to sintering during this treatment as a result of melting of Cr-, Mo-, C-rich regions above the 1235 °C eutectic temperature). The sintered material is then hot isostatically pressed to remove any remaining porosity and annealed at 1200 °C to minimize carbide networks by partial carbide dissolution. This results in increased ductility.

The strengthening mechanisms for the CoCrMo alloys include solid solution strengthening, dispersion strengthening (because of the fine $M_{23}C_6$ carbides and La and Al oxides, if present), carbide phase reinforcement [7], strain hardening (for the wrought alloys), and dislocation-grain boundary interactions. The coarse-grained cast structures exhibit ultimate and yield strengths ~ 860 and 550 MPa respectively with fatigue strengths ~250 MPa for samples in the solution-treated condition; fatigue strengths of 450 MPa have been reported using casting processes that result in ultrafine grain size [18]. The finer structure and strain hardening effects of the wrought alloys result in much higher ultimate tensile strengths (1330–1450 MPa), yield strengths (960–1000 MPa), and fatigue strengths (10^7 endurance limit ~ 690–830 MPa). These values are similar to those reported for the powder-made bar stock materials formed by hot isostatic pressing (HIP) [19].

To achieve secure implant-to-bone fixation without the use of acrylic bone cement, cast CoCrMo implant surfaces can be modified by either sintering CoCrMo alloy powders to the bone-interfacing surfaces, or otherwise texturing the surface (e.g. grit-blasting) [20, 21]. For the sintered coatings, typically, 250–350 μm size powders (−45/+60 mesh) are used to form porous coatings of approximately 50–70% density (i.e. vol. % porosity ~ 30–50%). Secure particle-to-particle and particle-to-substrate core bonding is achieved by sintering CoCrMo alloy powders at around 1300 °C for a period of 1 h or so. This high temperature sintering anneal significantly alters the microstructure and mechanical properties of both cast and wrought CoCrMo alloys. As noted previously, for cast alloys, localized melting of the Cr-, Mo-, C- rich interdendritic zones occurs at approximately 1235 °C, the eutectic temperature for the solute-enriched interdendritic region [16]. Upon

cooling, eutectic phase structures (γ-phase + $M_{23}C_6$ carbides + possibly some σ-phase) form inter- and intra-granularly (Fig. 1.12a, b). These eutectic structures form as networks at sinter neck regions and along the solid substrate grain boundaries where they form pathways for easy crack propagation thereby resulting in reduced ductility and fracture resistance of porous-coated implants (Fig. 1.12). This undesirable effect can be minimized through slow cooling from the normal sintering temperature (~1300 °C) to below the eutectic melting temperature (1235 °C) [18] thereby minimizing the amount of γ-phase + carbide eutectic formed at the eutectic temperature as predicted by the lever rule (see Fig. 1.10). While early use of sintered porous coatings was limited to cast CoCrMo compositions because of concerns of recrystallization and grain growth during sintering of wrought CoCrMo alloys leading to low strength, the development of high-C and dispersion strengthened wrought Co-based alloys with fine nonmetallic dispersoids throughout to inhibit grain growth (i.e. carbides or Al and La oxides) made it practical to porous coat these alloys and retain relatively small grains (60–150 μm size range). Further, the more homogenous compositions of the wrought alloy substrates reduce significantly the amount of $M_{23}C_6$-γ-phase eutectic formation. As a result, higher mechanical properties of wrought high-C Co alloy porous-coated samples can be achieved (fatigue strengths equal to 241 MPa compared to 207 for porous-coated cast samples [17]; La and Al oxide dispersion strengthened porous-coated samples are reported to have higher fatigue strengths equal to 345 MPa [19]).

Despite these developments aimed at improving mechanical properties of Co-based alloys, their use for making components subjected to high tensile and bending forces (e.g. femoral stem components of hip implants) has been reduced as a result of the increased use of Ti alloys. However, high-C CoCrMo continues to be used extensively for bearing components of modular hip replacements. However, as a result of increasing concern over Co (and Cr) ion release, ceramic component alternatives (Al_2O_3, Al_2O_3-ZrO_2, phase- stabilized ZrO_2) are increasing in popularity.

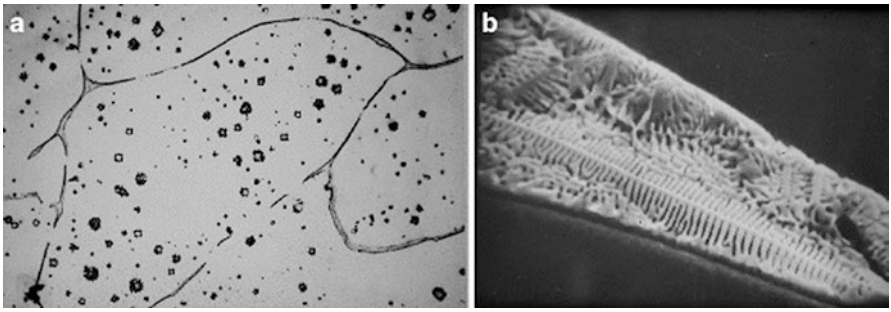

Fig. 1.12 Scanning electron micrographs of polished CoCrMo samples following a 1300 °C 1 h sinter annealing treatment followed by a normal furnace cool to room temperature showing (**a**) grain boundaries with eutectic structure ($M_{23}C_6$ + γ-phase primarily) and (**b**) higher magnification view of the grain boundary microstructure; the lamellar eutectic structure of $M_{23}C_6$ + γ-phase lamellae is clearly visible

A ZrO_2 surface-layered Zr-Nb alloy (described in a later section) represents a more recent alternative for hip and knee bearing surface applications.

1.9.2.3 Other Co-Containing Implant Alloys (ASTM F 562, F 90, F 563, F 1058)

While the CoCrMo alloys described above have represented the most common Co-based alloys used in orthopedics, other Co-containing alloys have been and continue to be used [9]. These are described briefly. All these contain alloying elements that significantly affect the nature of the fcc to hcp transformation of these alloys. This in turn has a strong effect on their properties. Cr, Mo, W, and Si are elements that stabilize the hcp phase while C, Ni, Mn, and Fe are fcc phase stabilizers. MP35N (F562 – Tables 1.5 and 1.6) contains 33–37 wt% Ni, an equal amount of Co and somewhat less Cr (19–21 wt%) compared with the F75 alloy. The high Ni content stabilizes the fcc phase so that at temperatures between 425 and 650 °C, a two-phase fcc (γ) + hcp (ε) equilibrium structure can form. However, mechanical working and the associated strain energy is required to nucleate the ε-phase at this lower temperature. The exact thermomechanical treatment used determines the size and distribution of the resulting hcp bands that form and, hence, the degree of strengthening due to the interaction of dislocations with the γ-ε interphase boundaries throughout the structure. To maintain acceptable corrosion resistance, MP35N has a higher Mo content than the CoCrMo alloys in order to compensate for its reduced Cr content. The higher Mo also can contribute to further strengthening since on annealing in the 425–650 °C range, an intermetallic compound, Co_3Mo precipitates within the hcp zones. As shown in Table 1.5, the MP35N can develop very high fatigue strengths, a feature that made it particularly attractive for forming hip implant components. However, concern over its high Ni content and the reported occurrence of Ni-sensitivity in a significant percentage of the general population has limited its use for joint replacement implants intended for long-term in vivo residence, although it remains popular for fabrication of fracture fixation (temporary) implants as well as conducting leads of cardiac pacing systems.

Other Co-based alloys that are used in implant applications include Elgiloy (ASTM F-1058) and the W-containing alloys (ASTM F-563) – (Tables 1.5 and 1.6). Elgiloy is renowned for its high spring-back qualities when highly cold-worked, a property that makes it attractive for fabrication of neurosurgical and vascular implants (neural aneurysm and microvascular clamps) as well as conducting leads for pacemakers. The W-containing CoCrNi alloy (ASTM F-563) has been used for making fracture fixation implants. These alloys are not as corrosion resistant as some of the Mo-containing Co-based alloys and they are strengthened primarily through work hardening. The common characteristic that all these Co- and CoNi-based alloys share in terms of response to thermomechanical treatment is the sluggish fcc to hcp transformation at relatively low transformation temperatures.

1.9.3 Titanium-Based Alloys

Titanium and its alloys have been used increasingly for fabrication of orthopedic implants (for fracture fixation and joint replacement applications) since the late 1960s. They are used virtually exclusively for forming endosseous dental implants (introduced for clinical use in the late 1970s), also a highly mechanically loaded application requiring implants with good fatigue resistance characteristics. (Additional information on properties and applications of Ti and Ti alloy implants can be found elsewhere [22]). The increasing use of Ti-based metals, in addition to their good fatigue resistance, is due to their excellent in vivo corrosion resistance, a feature related to the stable passive oxide layer (TiO_2) that rapidly forms, their lower elastic moduli compared to some other metallic biomaterials (100–110 GPa compared to 200–220 GPa for stainless steel and CoCrMo alloys) and their strong osseointegration tendency (i.e. development of close bone-to-implant apposition after short implantation periods). This latter characteristic represents an important advantage for permanent bone-interfacing implants.

Pure Ti is body-centered cubic (β-phase) at temperatures above 883 °C (the β-transus temperature) and hexagonal close-packed (α-phase) at lower temperatures (Fig. 1.13). Addition of most other elements stabilizes either one phase or the other. α-stabilizers include Al, O, N, and C while β-stabilizers are of two types, β-isomorphous (Mo, V, Nb and Ta) and β-eutectoid (Fe, W, Cr, Si, Ni, Co, Mn and H) [23, 24]. β-isomorphous Ti alloys have attracted interest for implant applications more recently because of the low elastic moduli possible with these alloys if appropriately processed. The elements Zr and Sn that are found in some Ti alloys are considered to be "neutral" alloying elements with no significant effect on either α- or β-phase stabilization.

The major disadvantage of Ti and its alloys is their poor wear resistance. This makes these metals unsuitable for load-bearing articulating surfaces without some type of surface modification to give greater wear resistance. This can be achieved through ion implantation (with N^+), TiN film application using physical vapor deposition (PVD) or other hard intermetallic compounds and methods of application. With the increasing use of modular hip implant designs this has become less of an issue since, with such designs, it is possible to combine a more wear resistant bearing component made of either a Co alloy, ceramic (Al_2O_3, Phase Stabilized ZrO_2) or ceramic surface-layered alloy (ZrO_2/Zr-Nb) with a high strength Ti alloy stem to form a replacement with good wear and fatigue resistance. The issue, nevertheless, remains a concern since modular designs of necessity have intercomponent junctions where relative micromovement and fretting can occur.

Porous Ti and Ti alloys formed as coatings for bone ingrowth and implant fixation can be formed by sintering Ti or Ti alloy powders or fibers (approximately 200–500 micron size) on Ti alloy substrates. This process (described below) is used to form porous-coated components of joint replacements and endosseous dental implants. A more recent method for forming porous coatings or structures uses an additive manufacturing technique (solid laser sintering – SLS) in which finer Ti

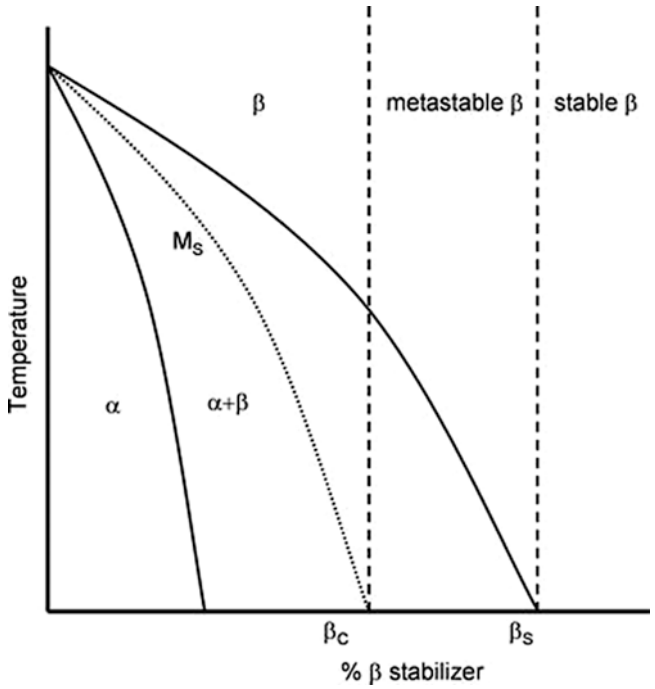

Fig. 1.13 Ti alloy equilibrium pseudobinary phase diagram. With increased β-stabilizer element additions, an (α + β) structure develops, above β_c a metastable β-phase is possible and above β_s only stable β-phase results. The *M_s line* represents temperatures below which martensite can form depending on the cooling rate used

powders (20–50 μm size) are applied layer by layer to form a porous coating or wholly porous parts intended for bone augmentation. The SLS treatment is usually followed by an anneal in order to increase sinter neck dimensions and strength while retaining the desired open-pored structure. Full density powder-made Ti or Ti alloy parts also can be made by selected laser melting (SLM) in which higher power lasers are used to fuse powders layer-by-layer to give desired finished forms after a post-SLM anneal. The additive manufacturing methods allow the formation of complex shapes according to prescribed designs.

1.9.3.1 Commercial Purity Ti

Unalloyed Ti (commercial purity – CPTi) can contain small amounts of interstitial elements including O, N, and H. While the quantities are small (Table 1.7), they affect mechanical properties through interstitial solid solution strengthening [7]. CPTi is available in four grades, Grade I having the lowest O content and yield strength but highest ductility and Grade IV the highest O content and strength but lowest ductility. Grade III and IV types are used for fabricating implants for

osteosynthesis applications (fracture/osteotomy stabilization and spinal fusion) but the mechanical strength (low fatigue strength in particular) precludes their use for joint replacement prostheses. CPTi (Grade III and IV) is used, however, for making endosseous dental implants where its characteristic of promoting rapid osseointegration makes it particularly attractive. This characteristic (osteoconduction) is believed to be due to OH^- ion formation on the passive TiO_2 layer and reaction of the resulting hydroxylated surface zone with bone mineral phase constituents (Ca^{2+} and $(PO_4)^{3-}$). Strengthening of CPTi is due to strain hardening during mechanical forming of parts, fine grain size, and interstitial solid solution strengtheners such as oxygen and nitrogen (Fig. 1.14). Formation of nanocrystalline Ti can be formed

Table 1.7 Examples of some Mg alloy compositions/mechanical properties being studied

Alloy ID	Nominal chemical composition (wt%)	Mechanical properties		
		σ_y (MPa)	σ_{ult} (MPa)	% elong
Al-free				
ZK30	Mg-3Zn-0.6Zr	215	300	9
ZK60	Mg-6Zn-0.6Zr	235	315	8
WE-43	Mg-4Y-3RE-0.5Zr (RE – Nd + other HRE)	160	260	6
JDBM-2	Mg-2.2Nd-0.1Zn-0.4Zr	309	276	34
–	Mg-3Nd-0.2Zn-0.4Zr	90	194	12
With Al				
AZ91	Mg-8Al-0.6Zn-0.04Si-0.22Mn	145	275	6
AZ31	Mg-3Al-1Zn-<0.05Si-0.2Mn	–	–	–
AM60	Mg-6Al-0.1Zn-0.35Mn	–	–	–

Note – Mechanical properties dependent on processing (i.e. as-cast, extruded, rolled, etc.)

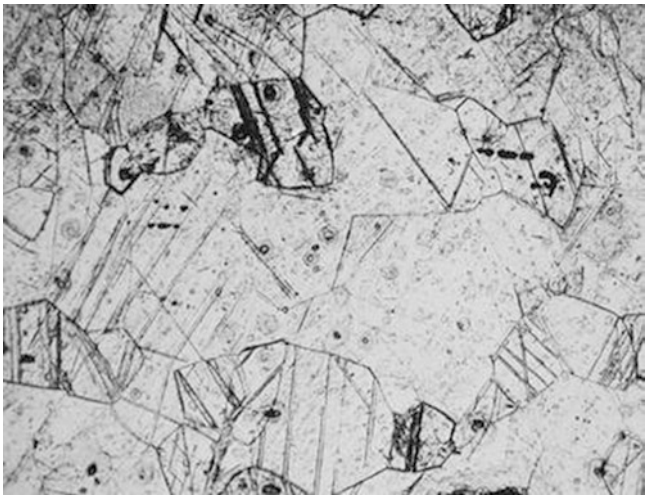

Fig. 1.14 Scanning electron micrographs of CP Ti. The structure is single phase. Grain and twin boundaries can be seen

with strengths approaching those of (α + β) Ti alloys (see next section) suggesting that pure Ti may be suitable for load-bearing applications thereby avoiding the need for potentially cytotoxic and allergenic elemental alloying additions [25]. Investigations of nanocrystalline titanium are ongoing.

1.9.3.2 (α + β) Ti Alloys

Alloying of Ti results in the formation of a two-phase (α + β) alloy with higher strength than microcrystalline CPTi while maintaining excellent corrosion resistance and osseointegration properties.

The (α + β) Ti alloy with the longest history of use for major load-bearing applications include Ti6Al4V, Ti6Al7Nb and Ti5Al2.5Fe. All three alloys behave equally well in clinical use. Bar stock of these alloys is formed by thermo-mechanical processing (mill-annealing) giving high fatigue strength materials (Table 1.8). Combined with their excellent corrosion resistance, implants made from these alloys display superior corrosion-fatigue properties compared to other metallic biomaterials. The mechanical properties of the (α + β) Ti alloys, fatigue strength in particular, are strongly dependent on the size and distribution of the α and β phase regions [10]. The so-called mill-annealing treatment (see below) results in the formation of small, equiaxed α-grains surrounded by fine β-phase particles (Fig. 1.15a). The mill annealing process involves mechanically working the alloy to a desired form at a temperature just below the β-transus temperature, rapid cooling (water quenching) to room temperature and then annealing to recrystallize the worked structure at around 750 °C (i.e. well within the α + β two-phase field). The rapid quenching treatment results in formation of α and a metastable α′-phase as well as the retention of some β-phase; α′ forms by a martensitic transformation mechanism.

Table 1.8 Dental casting alloys

Alloy type	**Ag**	**Au**	**Cu**	**Pd**	**Pt**	**Zn**		**Other**
Highnoble								
Au-Ag-Pt	11.5	78.1	–	–	9.9	–		Ir (trace)
Au-Cu-Ag-Pd-*I*	10.0	75.0	10.5	2.4	0.1	1.0		Ru (trace)
Au-Cu-Ag-Pd-*II*	25.0	56.0	11.8	5.0	0.4	1.7		Ir (trace)
Noble								
Au-Cu-Ag-Pd-*III*	47.0	40.0	7.5	4.0	–	1.5		Ir (trace)
Au-Ag-Pd-In	38.7	20.0	–	21.0	–	3.8		In 16.5
Pd-Cu-Ga	–	2.0	10.0	77.0	–	–		Ga 7.0
Ag-Pd	70.0	–	–	25.0	–	2.0		In 3.0
Base metal	**Ni**	**Cr**	**Co**	**Ti**	**Mo**	**Al**	**V**	**Other**
Ni-Cr	69–77	11–20	–	–	4–14	0–4	–	Fe, Be, Ga, Mn, B
Co-Cr	–	15–25	55–58	–	0–4	0–2	–	Fe, Ga, Nb, W, B, Ru
Ti	–	–	–	90–100			0–4	

Ref– Handbook of Materials & Med Devices – ed. JR Davis, ASM 2003

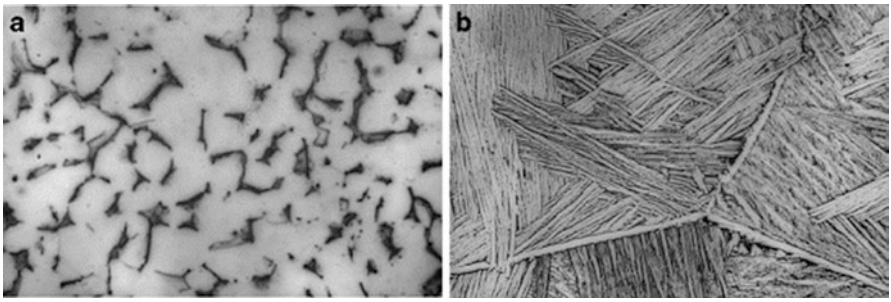

Fig. 1.15 Microstructure of Ti6Al4V alloy; mill-annealed condition (**a**) *light regions* are α-phase and *darker zones* are β-phase regions; β-annealed condition (**b**) showing the lighter appearing α-lamellae separated by β-phase lamellae. Note also the domain structures (zones within a single grain with α to β formed on different habit planes, i.e., same α to β orientation relation but involving planes in a different crystallographic orientation)

The 750 °C anneal, in addition to recrystallizing the worked structure, also results in the transformation of α′ to the stable α-phase. The amounts of α and β, as well as the size and distribution of these phases is dependent on the extent of mechanical deformation during component forming near the transus temperature, the exact forming temperature and the recrystallization treatment. Fatigue strengths greater than 650 MPa (10^7endurance limit) can be achieved.

The excellent corrosion resistance of Ti6Al4V makes it an attractive choice for forming high surface area, porous-coated orthopedic implants either by sintering Ti or Ti alloy powders or fibers to the surface of machined substrates, or alternatively, by additive manufacturing (SLS). Textured surfaces formed by depositing surface layers by plasma spray methods are also possible. Porous coatings formed by sintering involve sintering in a high vacuum or other nonoxidizing atmosphere at temperatures ≥ 1250°C for 1 h or so followed by furnace cooling to room temperature. This so-called β-anneal treatment results in a microstructure consisting of a lamellar (α + β) structure with "colonies" of lamellae forming within prior β grains (Fig. 1.15b). Because of the higher annealing temperature within the β-phase field (more than 250 °C above the α-β transus temperature), large β grains form. The "colonies" that form throughout the structure represent zones in which the α and β lamellae are oriented in different directions but all with a common crystallographic α-to-β orientation relation (i.e. lamellae form on common "habit" planes in the different colonies). The presence of these colonies and colony boundaries contributes to the strengthening of the alloy. However, the fatigue strength of the β-annealed samples is somewhat lower than for mill-annealed samples (i.e.10^7 fatigue endurance limit of smooth-surfaced β-annealed samples ~ 550 MPa compared to 620 MPa for mill-annealed samples) [10, 26]. Of greater consequence to fatigue strength is the effect of porous coatings or textured (unsmooth) surfaces per se. Their presence results in a reduction of fatigue strength to about a third (i.e. from 600 MPa to approximately 200 MPa) [26]. This is due to the notch fatigue sensitivity of hcp metals in general and specifically to Ti and other α-phase-containing Ti alloys. The

sinter neck–substrate junctions of the sintered porous layer represent stress concentrators at which fatigue can more readily initiate. Design and use of porous-coated Ti6Al4V components must take into consideration this reduced fatigue strength. Some femoral hip stem components are made with porous coatings, on all but the lateral stem surface which is kept relatively smooth since the highest tensile stress primarily responsible for fatigue crack initiation is expected to occur at this surface during normal functional loading of implants. Plasma spray deposition of Ti to form a textured surface suitable for cementless implant fixation can occur without significantly altering the mill-annealed implant substrate microstructure since the temperature within the alloy bulk remains low. Nevertheless, a similar reduction in fatigue strength occurs since the resulting surface is irregular with many sites for surface stress concentration.

1.9.3.3 β-Ti and Near β-Ti Alloys

These alloys have higher levels of β-stabilizing elements, Mo displaying one of the strongest effects. They are characterized by a Mo equivalent > 10. This is calculated by using different weighting factors for the elements added in forming the Ti alloy (i.e. Mo equiv = 1.0 (wt% Mo) + 0.67 (wt% V) + 0.44 (wt% W) + 0.28 (wt% Nb) + 0.22 (wt% Ta) + 2.9 (wt% Fe) + 1.6 (wt% Cr) + … [27]). While the Young's moduli of Ti and the (α + β) Ti alloys are significantly lower than those of CoCrMo or stainless steel alloys (~110 compared to 220 and 200 GPa, respectively), they nevertheless are 5–10 times greater than the modulus reported for cortical bone (10–20 GPa). The issue of stress shielding of bone next to well-fixed CPTi or (α + β) Ti alloy implants is a concern in the case of long-term load-bearing implant use (although less so than with the higher modulus Co-based or stainless steel alloys). β and so-called near-β Ti alloys, if appropriately processed, exhibit significantly lower elastic moduli (values as low as 44–51 GPa for water-quenched and cold-worked Ti-13Nb-13Zr, a near-β alloy [32]). These alloys if properly processed can display good formability, high hardenability, excellent corrosion resistance, and better notch sensitivity than the (α + β) Ti alloys. Annealing results in higher strength as a result of precipitation strengthening but this also results in an increase in modulus [24].

β-Ti alloys are characterized by retention of 100% β-phase on cooling from above the β-transus [27]. Considering the pseudobinary phase diagram of Ti + β-stabilizer alloying additions (Fig. 1.13), a metastable β-phase is retained on cooling from above the β-transus if the β-stabilizer content is greater than β_c and less than β_s. For levels greater than β_s, β-phase represents the equilibrium structure. The metastable β structures are characterized by low elastic modulus (55–75 GPa) but relatively low fatigue strength (e.g. 10^7 fatigue endurance strength ~ 265 MPa for the Ti-35Nb-5Ta-7Zr alloy (TNZT) – Table 1.8). As noted above, annealing the metastable β in the two-phase (α + β) field region results in some α-phase precipitation and an increase in strength but also a rise in elastic modulus to values approaching or just above 100 GPa (dependent on the amount of α-phase that forms).

Ti-13Nb-13Zr is an example of a so-called near β-Ti alloy [28]. Rapid cooling (water quenching) this alloy results in suppression of the β-transus temperature to a low enough temperature (< 575 °C) to cause formation of acicular α′ martensite, an hcp phase formed by a displacive transformation. This structure is characterized by a Young's modulus ~ 64–77 GPa (Table 1.8). Subsequent annealing in the (α + β) two-phase field (500 °C for 6 h – an aging heat treatment) causes the acicular α′ to coarsen and fine β-phase precipitates to form throughout, resulting in higher strength (because of precipitation strengthening) with an associated increase in elastic modulus to about 81 GPa. Heavy cold-working of α′ martensite is possible and results in the formation of a lower modulus material (~ 45 GPa) with strength even greater than water-quenched and precipitation hardened material while maintaining good ductility. Surface hardening for improved wear resistance can be achieved by aging (at 500 °C, for example) in an oxygen-containing environment [28]. This is due to the formation of a hard surface oxide layer as well as interstitial solid solution strengthening of the subsurface region (diffusion hardening).

1.9.4 Zr-Nb Alloy

Zirconium, like titanium, is a highly reactive metal and will form a dense cohesive surface oxide layer (ZrO_2) spontaneously on exposure to an oxygen-containing environment. In addition to its corrosion protection, ZrO_2 is very hard and can be used to form a good wear resistant surface assuming sufficient thickness. A Zr-2.5Nb alloy, developed initially for nuclear industry applications, when annealed in an oxygen-containing atmosphere at 500 °C develops a relatively thick (5 μm) monoclinic ZrO_2 layer over the alloy substrate [29]. The underlying alloy consists of a two-phase (α + β) alloy structure with the dominant phase being hcp α with a small percentage of bcc β phase distributed throughout. The 500 °C surface oxidation treatment also results in interstitial solid solution strengthening and possible internal oxidation resulting in dispersed oxide particles forming (dispersion strengthening) both of which result in increased strength. Surface oxidized Zr-Nb alloy is used for making orthopedic components that are intended to resist wear (such as femoral head components of hip implants and knee implant components). The structure offers the advantage over whole ceramic components of reduced risk of catastrophic fracture since the ZrO_2 layer is reinforced by a Zr-Nb alloy body. Clinical outcomes of this novel system are being followed currently [30, 31].

1.9.5 Ni-Ti Alloys (Nitinol)

The equiatomic Ni-Ti alloy (Nitinol) is used currently in certain orthopedic, dental and cardiovascular applications [32]. The shape-memory effect that the alloy displays as well as its reported good corrosion resistance, (the result of a TiO_2 passive

surface layer), and its pseudoelastic property (Young's Modulus, E ~ 28–41 GPa for the martensitic phase) has attracted interest in the biomaterials field in recent years. In vivo studies have indicated that the alloy is biocompatible despite its high Ni content [33, 34]. However, the concern over long-term consequences of even minor amounts of Ni ion release are likely to limit its use for production of intended permanent implants (e.g. joint replacements). Published reports indicate that with proper processing, corrosion properties comparable to 316L stainless steel are achievable [35–37] so that use in limited-term applications such as fracture fixation is practical.

The shape memory effect is due to the thermoelastic martensitic transformation that occurs with Ni-Ti shape memory alloys. Cooling from a high temperature, (i.e. above body temperature for some Ni-Ti-based alloys), to a lower temperature results in the transformation of the austenite phase (an ordered intermetallic compound with a distorted bcc unit cell structure resulting from the ordering of Ni and Ti atoms giving a so-called B2 unit cell structure) to martensite. The transformation is isothermal but most of the phase change occurs over a fairly narrow temperature range between M_s and M_f. The temperature at which the austenite-to-martensite (or reverse) transformation occurs is dependent on the exact composition of the alloy. The Ni-Ti intermetallic compound, unlike most other intermetallic compounds, has a moderate range of solubility for excess Ni or Ti as well as other elements and this allows "engineering" of the critical transformation temperatures (M_s, M_f, A_s and A_f). Thus, it is possible to develop shape memory alloys (SMAs) with transformation temperatures corresponding to body temperature. The austenite-martensite transformation can also be induced by mechanical deformation. While the overall change in shape due to cooling of austenite is minor due to the formation of a number of counteracting twin variants that develop thereby minimizing the overall shape change, as discussed previously, stress-induced martensite results in the development of a preferred twin variant. This involves a so-called *detwinning* reaction in which a twin variant preferentially oriented to the principal strain direction grows at the expense of other twins resulting in significant volume and net shape changes. If this shape change is constrained, appreciable stress can develop in the material and this stress can be transferred to adjacent tissues (assuming secure anchorage of the Ni-Ti component). By way of example, a fracture fixation staple made of Nitinol, if deformed in the martensitic state (i.e. at room temperature) and then used to unite fractured bone fragments, will exert a strong force pulling the fragments together as it warms up in the body to above its A_f temperature and reverts to its prior austenitic shape. Other applications have been proposed in orthopedics including other fracture fixation devices, spinal rods for treatment of scoliosis, cages for use during spinal fusion and even self-locking joint replacement components [36].

Wires formed of Nitinol are used currently in orthodontics although, in this application it is the alloy's pseudoelasticity that makes it so attractive. SMAs are also used for cardiovascular stents where the pseudoelastic feature facilitates stent expansion/deployment following insertion into an artery. The ability to tailor the transformation temperature of Ni-Ti alloys through slight alloying modifications as noted above is important since this allows the formation of materials and devices

displaying this superelastic behavior at a desired temperature corresponding to expected in-service conditions. Orthodontic wires formed from a Ni-Ti-based alloy are useful because of the large "working range" that these wires provide during force application for tooth re-positioning.

The stress-strain curves for NiTi alloys are dependent on the M_s temperatures with yield strengths and fatigue strengths increasing with decreasing M_s. Accurate determination of alloy transformation temperatures is critical for the design of components and prediction of performance.

1.9.6 Tantalum

Porous tantalum foam structures are used as bone augmentation templates. Ta has been considered for many years to be biocompatible as a result of the stable tantalum oxide (Ta_2O_5) that forms on its surface. The metal has been used in other implant applications such as implantable cranial plates for years. Ta foam structures for bone augmentation [38] are formed by chemical vapor deposition (CVD) and infiltration (CVI) of tantalum onto vitreous carbon lattice structures, thereby building up Ta struts of desired dimensions. The vitreous carbon lattices are formed by pyrolysis of thermosetting polymer foams. The Ta deposited onto the carbon filamentous structures to a desired thickness giving an open-pored Ta structure (approximately 99 wt% Ta + 1 wt% vitreous carbon) (Fig. 1.16). The dimensions of the Ta struts are controlled by the amount of Ta applied and this determines the mechanical properties of the foam. Structures with compressive and tensile strengths ~60 and 63 MPa respectively and compressive fatigue strengths ~23 MPa (5×10^6 endurance limit) have been reported [38]. Continuous interconnecting pores, or cells, about 550 μm in size, are formed and elastic and strength properties similar to those of cancellous bone result. Animal studies [39] have demonstrated the effectiveness of these structures for bone augmentation purposes. While the as-made mechanical properties of

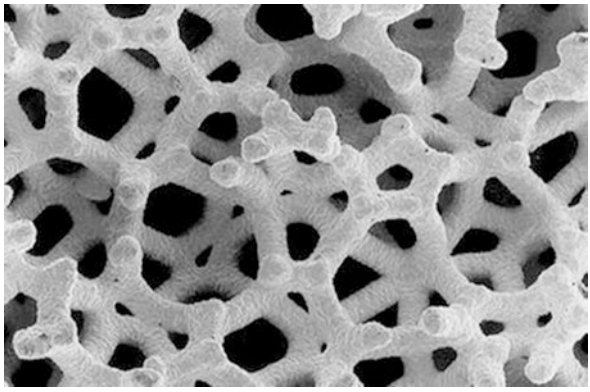

Fig. 1.16 Scanning electron micrograph of open-pored Ta foam. (Courtesy Dr JD Bobyn)

the foams are low, they are considered sufficient to allow bone ingrowth and filling of the structures after which bone is expected to share the load-bearing requirements.

1.9.7 Platinum, Platinum-Iridium

Electrodes used for neuromuscular stimulation require the use of materials that are corrosion resistant under extreme voltage potential and charge transfer conditions. The noble metals (Pt and Pt-Ir alloys) satisfy these conditions and are the principal materials used for making electrodes for electrical stimulation and sensing purposes. The Pt-Ir alloys (10–30 wt% Ir) offer the advantage of higher mechanical properties (scratch resistance) compared with unalloyed Pt because of solid solution strengthening as well as the mechanical working during part formation. Other noble metals that have been used for fabricating electrodes for electrical stimulation include rhodium, gold and palladium but these are not used extensively for these applications [9]. Some non-noble metals have also been used (stainless steel, Ti, Co-based alloys) but these are more prone to corrosion (passive film breakdown occurs at potentials above the breakdown potential). Hence, these alloys are not as suitable as the noble metals.

Conducting leads used with the electrodes are made of metals that in addition to being corrosion resistant and electrically conductive, must display high flexural fatigue strength. Helically coiled lead wire designs are used currently to achieve good lead flexibility and to minimize local strains during flexing thereby improving fatigue characteristics. Stainless steel, wrought CoCrMo alloy (Elgiloy) and Co-Ni alloys (MP35N) are popular choices for conducting leads [9].

A Pt-Cr steel (33 wt% Pt) has been reported for forming vascular stents [40]. The greater radiopacity of the alloy (due to the high atomic weight Pt) offers advantage in imaging the stent during insertion and deployment.

1.9.8 Magnesium Alloys

Magnesium is a biodegradable metal (in vivo corrosion and acceptable biocompatibility of it and its degradation bi-products – Mg(OH) and H_2 gas). Mg is also an essential nutritional element with a relatively high recommended maximum daily intake for adults (240–420 mg/day). This characteristic as well as its relatively low elastic modulus ($\approx$ 45 GPa) has sparked interest in Mg as a metal for cardiovascular (stents) and orthopedic (fracture fixation) applications [41, 42]. Unfortunately, unalloyed Mg is characterized by low strength and it corrodes too rapidly both in vitro and, more significantly, in vivo with associated unacceptably rapid loss in mechanical strength and stiffness, two important and necessary characteristics for stents and

fracture stabilization devices. In addition, the rapid corrosion of Mg in aqueous-containing environments and the resulting hydrogen gas evolution can cause unacceptable biological responses including inhibition of bone formation during fracture healing and excessive neointimal formation with an associated inflammatory reaction. Thus, alloying of Mg for increased strength and, more importantly, lower corrosion rates is crucial for its acceptability as a useful biomaterial. Many studies have reported on different alloying strategies to achieve adequate mechanical and corrosion characteristics. Included have been investigations of Al-containing Mg alloys but because of the reported neurotoxic effects attributed to Al, interest has focused more on Al-free Mg alloy compositions. Included are a number of multicomponent alloy systems based on extension of Mg-Zn, Mg-Zr, and Mg-RE (Rare Earth) binary systems through the addition of other elements [42]. Some of the Mg alloy compositions that have been and continue to be investigated are shown in Table 1.7. Increased mechanical strength through the alloy additions are attributable to solid solution strengthening and precipitation strengthening and fine grain size – (Ca and Zr additions are particularly effective grain refiners). Examination of the binary phase diagrams for Mg-Zn, Mg-Zr and Mg-RE show a limited solubility of the primary alloying element with Mg thereby contributing to solution strengthening but also the possible formation on heat treatment of precipitates, secondary phases and stacking faults, all of which serve to inhibit dislocation glide giving higher yield strengths. In addition, minor element additions (e.g. Ca, Si, Mn, Y, Sr, Nd, Gd, Cd, and other REs) may result in the formation of LPSO structures in some alloys *(LPSO = long-period stacking-ordered*) and intermetallic compounds which contribute to higher yield strength [43]. Mg alloy development for biomedical implant applications, at present, remains experimental. While some progress has been made in improving corrosion resistance thereby yielding lower degradation rates, this continues to be the major challenge in development of clinically acceptable, biodegradable Mg-based implants. The clinical use and comparison of biodegradable/absorbable Mg alloy (MgYREZr alloy) compared with a polylactide-glycolide (PLA-PGA) commercially available bioabsorbable screw for orthopedic applications (interference screws) has been reported and the results indicate the advantage of higher strength Mg-based screws compared with the PLA-PGA screw. In another reported clinical application, a commercial MgYREZr alloy screw was reported to be as effective as a commercial Ti screw for treatment of foot (hallux valgus) deformities [41, 42]. Biodegradable Mg-RE alloy stents implanted in patients have been reported with favorable response and safe degradation of the devices within a 4-month period [44]. The issue of corrosion rate remains a concern, however, as does the long-term biocompatibility of the implant degradation products. While many reports have indicated the noncytotoxic character of some of the elemental additions referred to above, investigations continue to both develop slower degrading Mg alloys and structures (protective coatings are being explored) and to gain a better understanding of the long-term consequences of the in vivo effect of released alloying additions.

1.9.9 Dental Alloys

Metals are used in dentistry for fillings in decayed teeth (dental amalgams), fabricating crowns and bridges (noble and base metal alloys), partial denture frameworks (base metal alloys), orthodontic wires and brackets (stainless steel, Ti alloys and Ni-Ti alloys), and dental implants (CPTi and Ti6Al4V). As in orthopedic applications, the major advantage of metal for these dental applications is the high intrinsic strength and fracture resistance of this class of materials. Biocompatibility is again an important requirement since these materials also contact body tissues (tooth structure, soft supportive tissues) often for the remainder of a patient's lifetime although the relative ease of accessibility after placement relaxes the biocompatibility requirement considerably. A number of the metals already described (as indicated above) find application in dentistry. Dental implant materials with requirements very similar to materials used for orthopedic joint replacement implants are made almost exclusively from Ti and Ti6Al4V. Orthodontic wires and brackets are made of stainless steel (types 302, 303, 304 and 305), CoCrNiMo alloys (Elgiloy), β-Ti, and Ni-Ti alloys (because of the low elastic modulus, high yield strength, and consequently large working range, a desirable characteristic for this application).

1.9.9.1 Dental Amalgams

Dental amalgams are formed by adding Hg to dental amalgam alloys (alloys containing Ag, Cu, and Sn plus some other minor elemental additions) (amalgamation process) [45]. Dental amalgam alloys are either low (Cu < 6 wt%) or high Cu-containing (Cu > 6 wt%), the latter being favored because it avoids the formation of an undesirable Sn-Hg phase (γ_2) that is susceptible to rapid corrosion and results in lower strength properties of amalgams. Dental amalgam alloys are formed as powders either by lathe cutting Ag-Cu-Sn alloy billets (resulting in irregular particles – i.e. machining chips) or by atomization (to give spherical powders). Subsequent mixing of these alloys with mercury results in their partial dissolution, complete consumption of the liquid Hg and the subsequent formation of a number of intermetallic compounds (Ag_3Sn, Ag_2Hg_3, $Sn_{7\text{-}8}Hg$, Cu_3Sn, Cu_6Sn_5) due to the Hg-dental amalgam alloy reactions and the condensation of the initial "plastic" mass. During the reaction, the partially reacted powder can be manipulated to fill a tooth cavity. The final amalgam restoration, after virtual completion of the amalgamation reaction, exhibits reasonable mechanical properties. While susceptible to corrosion in the oral environment, buildup of the corrosion product serves to limit the rate of further corrosion and to form an acceptable marginal seal at the amalgam-tooth interface. The major advantage of this material is its easy in situ formability to a desired shape. Concerns related to Hg toxicity have been raised but, to date, these have not been proven to be valid although the issue remains controversial.

1.9.9.2 Dental Casting Alloys – (Au-Based, Co-Based, Ni-Based, Ti-Based)

Dental casting alloys are used for making dental bridges, crowns (with porcelain fused to a metal substrate), inlays, onlays, and endodontic posts. Both noble and non-noble (base) metal alloys are used to form these often-complex shapes. Requirements include sufficient strength, toughness, wear resistance, corrosion resistance and biocompatibility. The noble metal alloy compositions are primarily Au- or Pd-based with alloying additions of Ag, Cu, Pt, Zn and some other trace elements. These can be divided into "high noble" alloys (noble metal content ≥ 60 wt%) and "noble" alloys (noble metal content ≥ 25 wt%) [9]. Some of the Au-based alloys are heat treatable with precipitation hardening or order-disorder reactions (similar effect to precipitation hardening for some alloys) contributing to increased strengths. The base (non-noble) metal alloys contain ≤ 25 wt% noble metal elements and are either CoCr or NiCr alloys (Table 1.8). Cast Ti components for crowns, partial and complete dentures, while limited because of difficulties associated with casting because of the high melting point of Ti (compared to Au-based dental alloys), its high reactivity, difficulty in surface finishing and other problems, can be made (using special vacuum melting and casting equipment) but it is not common. Such cast Ti components are useful, however, for individuals with allergies to Ni- or Co-based alloys. Ti-based alloys are also possible including Ti6Al4V, TiCuNi, TiV, TiCu, TiPd, and TiCo alloys (some of these are still in the experimental stage of development). To satisfy aesthetic requirements for dental crowns, porcelain-fused-to-metal (PFM) restorations are made with the silicate-based porcelains being bonded to a cast metal substrate. Attainment of good bonding of porcelain to the dental alloy substrate is achieved through micromechanical interlock and interfacial chemical reactions, the latter usually involving a substrate surface oxide reacting with the porcelain coating. Compatible thermal expansion coefficient of metal coping and porcelain cladding materials is important to ensure slight residual compressive stresses in the porcelain for inhibition of cracking. Corrosion resistance of the underlying dental alloy is necessary to avoid unacceptable staining and discoloration of a PFM crown.

1.9.9.3 Wrought Dental Alloys

As noted above, wrought stainless steel, CoCrNi (Elgiloy), β-Ti, and Nitinol alloys are used for making orthodontic wires where high yield strength and preferably low elastic modulus provides high "working range" characteristics. The requirement of low elastic modulus favors the selection of β-Ti and Ni-Ti alloys for orthodontic wires although all four alloys are used at present. Wire drawing procedures result in strain hardening and high yield strengths but can be performed such that the wires are sufficiently ductile to allow their manipulation and shaping during placement.

CPTi and (α + β) Ti alloys (Ti6Al4V) are used for making endosseous dental implants. These components are prepared by machining shapes from bar stock

followed by appropriate surface finish operations. In order to achieve more rapid osseointegration, implant surfaces are modified using plasma spray coating, acid etching, grit blasting, laser ablation, anodization, microarc oxidation, anodic spark deposition, or addition of metal powder sintered surface layers. These additional treatments can result in final products with either mill-annealed microstructures or, as in the case of Ti6Al4V implants with sintered surface layers, β-annealed structures. In addition to geometric or topographic surface modifications, surface chemical modifications (e.g. addition of calcium phosphate surface layers using one of a number of possible methods) are used to promote increased osteoconductivity resulting in faster rates of osseointegration.

1.10 New Directions

While progress in metallic implant manufacture and more knowledgeable selection of materials have resulted in safer and more effective implants over the past 50 years or so, a number of limitations and concerns persist or have arisen with changing social situations. With increasing life expectancies coupled with more active lifestyles for the aged, has come an increasing need for further advances in biomaterials and methods for implant fabrication. Metals are expected to continue to play a major role in these advances both alone and in association with other biomaterials (i.e. polymers, ceramics, composites). One objective for the future is the development of more biocompatible and bioactive systems to promote a preferred host response. Surface modification of metal implants to this end has been explored during the past few decades and these efforts are expected to continue with increasing focus on the incorporation of biologics to promote desired responses (e.g. enhanced osseointegration, infection resistance, biocompatibility). Improving engineering properties (e.g. wear, fretting-corrosion, fatigue resistance) of implants through surface modifications will also continue with further innovations using novel materials and methods.

Development of biodegradable metals of initial strength suitable for high load-bearing applications remains a goal for biomaterials researchers with particular interest in Mg alloys developed for osteosynthesis uses. Investigations of Mg alloys could be extended for their use as temporary, open-pored scaffolds or other porous forms serving as templates for guided tissue/bone regeneration. A major issue to be dealt with, in addition to ensuring suitable mechanical properties and corrosion rate, is the assurance that degradation products are biocompatible and can be safely expelled from the body [46].

The increasing emphasis on minimally invasive surgery using diminutive implants represents another area for development of improved metallic biomaterials. Smaller-sized implants subjected, therefore, to higher stresses will need to be made of materials displaying higher mechanical strengths, particularly fatigue strength. Nanocrystalline metals may satisfy this requirement. Studies in other engineering fields have shown that nanocrystalline metals (crystal size < 100 nm) can

give higher yield, ultimate and fatigue strengths as well as higher hardness compared to conventional microcrystalline metals [47–49]. This improvement in mechanical properties appears related to the nano-sized grains and resulting more uniform dislocation distribution throughout the structure as well as inhibition of extensive dislocation glide and interactions with other dislocations due to the small grain size. Plastic deformation of nanocrystalline metals, rather than being due to dislocation movement and interactions with other dislocations or lattice defects as occurs with conventional micro-structured metals, is due to a great extent to grain boundary sliding [47]. Studies on optimizing structures to achieve high strength and hardness with a required degree of ductility have indicated a benefit of bimodal grain size distributions, with nanocrystalline and some microcrystalline component [50]. Glassy metals, wholly amorphous structures, formed by very rapid solidification of molten metals also display high strength and corrosion resistance. However, formation of glassy metals is limited to certain alloys with equilibrium phase diagrams displaying low temperature eutectic points and to processing of thin tapes and films for which very rapid cooling is practical. Thus, their application as biomaterials is limited at best and more likely, impractical unless methods for forming amorphous (glassy) surface layers securely bonded to crystalline metal substrates can be developed. The issue of long-term stability of nanocrystalline metals is a concern since studies (nonbiomaterial-related) have shown that with repeated cyclic loading, localized nanocrystalline zones can experience grain growth eventually resulting in micron-sized grains where fatigue crack initiation occurs [51]. Fatigue crack propagation, following initiation, in nanocrystalline metals is more rapid compared to conventional micron-sized polycrystalline metals since microstructural barriers to propagating cracks (e.g. precipitates, second-phase boundaries, stacking faults) are infrequent [49]. Nanocrystalline metals also appear to exhibit better corrosion resistance than microcrystalline metals. It is suggested that this is due to the reduced electrochemical potentials between anodic and cathodic zones within nanocrystalline structures by virtue of their smaller grains and greater grain boundary volume [52]. The anodic intergranular and cathodic intragranular regions are less distinct in the refined structures so that the driving potential for corrosion is reduced. More rapid re-passivation of disrupted passive oxide layers also occurs by virtue of the higher diffusion rates within the extensive grain boundary regions. The greater corrosion resistance in combination with higher hardness suggests the potential usefulness of nanocrystalline metals in forming components of modular implants where fretting-corrosion is a major concern. Formation of nanocrystalline bulk metals can be achieved by a number of methods including severe plastic deformation (SPD), high-energy ball milling, electrochemical means through formation of nonmetallic (e.g. oxide) nanostructured coatings by anodization or micro-arc oxidation (MAO), physical and chemical vapor deposition (PVD, CVD) [47, 48] and very rapid solidification (melt cooling rates ~ 10^6C°/s). All these methods are currently being investigated for forming nanostructured implants. In addition to developing very fine grain structures, some of these approaches also offer the possibility of developing unique non-equilibrium phases at room temperature. The higher strengths attributed to nano-structured metals may allow the use of unalloyed

nanocrystalline or ultrafine-grained (UFG – 100−1000 nm grain size) metals in certain high load-bearing situations that would otherwise rely on alloying. This would allow the avoidance of certain alloying elements that may be cytotoxic or allergenic (e.g. Al, V, Ni for Ti and NiTi alloys have been so suggested) [47]. Determination of properties of novel compositions and structures formed by these methods, (including, most importantly, their biocompatibility characteristics), represents an important area for future metal biomaterials research. In addition, studies are needed to characterize long-term mechanical behavior (fatigue, wear, fretting resistance) of nanocrystalline and ultrafine-grained (UFG) metals. The effects on mechanical performance (fatigue resistance) and structural stability of these metals following long-term repeated loading in an in vivo environment must be well understood prior to broad clinical acceptance of nanostructured and ultrafine-grained metallic implants in major load-bearing applications.

Additive manufacturing (AM) methods (selected laser melting, SLM) have been applied recently to formation of complex metallic forms including Ti alloy and stainless steel components for various engineering applications. In combination with appropriate imaging techniques, AM may be suitable for preparing custom-made, one-off implants. High performance parts so formed would most likely need to be post-SLM annealed or treated by hot isostatic pressing in order achieve suitable mechanical properties through elimination of residual pores and voids that might have resulted during the layer-by-layer SLM processing. The possible presence of even a very small percentage of such structural defects (including oxide inclusions that may be introduced during post-SLM annealing) could severely affect fatigue properties [53]. Appropriate designs accounting for experimentally determined mechanical properties and quality assurance procedures of final implant components to ensure that defects, if present, are below a critical size for the expected loading conditions should be used. Selected laser sintering (SLS) is similar in principle to SLM but with lower power and energy densities being used thereby resulting in interparticle sinter neck formation. In this way, porous structures with preferred characteristic % porosity, pore size, porous geometry can be made. As with SLM-made parts, post-SLS annealing will likely be required to ensure acceptable quality (i.e. strength and geometry) of the porous structures.

This article has been limited to discussion of metals used for forming bulk fully dense or porous implant components only. Metal elements other than those referred to in this chapter are also being investigated for the formation of novel systems for diagnostic and therapeutic uses in the medical field. The issue of assurance of long-term safety and biocompatibility of all these metal-containing systems is of paramount importance.

For the fully dense and porous metals, particularly those intended for major load-bearing and long-term performance, appropriate selection and processing is a necessary requirement in implant design and fabrication. An understanding of metal processing and how this influences properties and, ultimately, implant performance in patients is most important. This represents the underlying theme of this chapter.

References

1. Ashby MF, Jones DR. Engineering materials 1. An introduction to their properties and applications, and 2. Engineering materials 2. An introduction to microstructures, processing and design. Oxford: Pergamon Press; 1980.
2. Newey C, Weaver G. Materials principles and practice. London: Butterworth Scientific Ltd; 1990.
3. Abbaschian R, Abbaschian L, Reed-Hill RE. Dislocations and plastic deformation and elements of grain boundaries, physical metallurgy principles. 4th ed. Stamford: Cengage Learning; 2009. p. 119–93.
4. Wayman CM, Duerig TW. An introduction to martensite and shape memory. In: Deurig TW, Melton KN, Stockel D, Wayman CM, editors. Engineering aspects of shape memory alloys. London: Butterworth-Heinemann; 1990. p. 3–20.
5. Abbaschian R, Abbaschian L, Reed-Hill RE. Deformation, twinning and martensitic reactions, physical metallurgy principles. 4th ed. Stamford: Cengage Learning; 2009. p. 521–61.
6. Pilliar RM. Modern metal processing for improved load-bearing surgical implants. Biomaterials. 1991;12:95–100.
7. Kilner T, Laanemae WM, Pilliar RM, Weatherly GC, MacEwen SR. Static mechanical properties of cast and sinter-annealed cobalt-chromium surgical implants. J Mater Sci. 1986;21:1349–56.
8. Williams DF. Chapter 6: corrosion of orthopedic implants. In: Williams DF, editor. Biocompatibility of orthopedic implants, vol. 1. Boca Raton: CRC Press; 1982.
9. Davis JR, editor. Handbook of materials for medical devices. Materials Park: ASM International; 2003.
10. Pilliar RM, Weatherly GC. Developments in implant alloys. CRC Crit Rev Biocompat. 1986;1:371–403.
11. Narayan R. Medical applications of stainless-steel. In: Narayan R, editor. ASM handbook, Vol 23, Materials for medical devices. Materials Park: ASM International; 2012. p. 199–210.
12. Sigwart U. Endoluminal stenting. London: WB Saunders Co Ltd; 1996.
13. Pilliar R, Ramsay SD. Cobalt-base alloys. In: Narayan R, editor. ASM handbook, Vol 23, materials for medical devices. Materials Park: ASM International; 2012. p. 211–22.
14. Tandon R. Ne-shaping of Co-Cr-Mo (F75) via metal injection molding. In: Disegi JA, Kennedy RL, Pilliar R, editors. Cobalt-base alloys for biomedical applications, ASTM STP 1365. West Conshohocken: American Society for Testing and Materials; 1999. p. 3–10.
15. Taylor RNJ, Waterhouse RB. A study of aging behaviour of a cobalt based implant alloy. J Mater Sci. 1983;18:3265.
16. Kilner T, Pilliar RM, Weatherly GC, Allibert C. Phase identification and incipient melting in a cast Co-Cr surgical implant alloy. J Biomed Mater Res. 1982;16:63.
17. Wang KK. A dispersion strengthened Co-Cr-Mo alloy for medical implants. In: Disegi JA, Kennedy RL, Pilliar R, editors. Cobalt-base alloys for biomedical applications, ASTM STP 1365. West Conshohocken: American Society for Testing and Materials; 1999. p. 89–97.
18. Berlin RM, Gustavson LJ, Wang KK. Influence of post processing on the mechanical properties of investment cast and wrought Co-Cr-Mo alloys. In: Disegi JA, Kennedy RL, Pilliar R, editors. Cobalt-base alloys for biomedical applications, ASTM STP 1365. West Conshohocken: American Society for Testing and Materials; 1999. p. 62–70.
19. Mishra AK, Hamby MA, Kaiser WB. Metallurgy, microstructure, chemistry and mechanical properties of a new grade of cobalt-chromium alloy before and after porous-coating. In: Disegi JA, Kennedy RL, Pilliar R, editors. Cobalt-base alloys for biomedical applications, ASTM STP 1365. West Conshohocken: American Society for Testing and Materials; 1999. p. 71–88.
20. Pilliar RM. Powder metal-made orthopaedic implants with porous surfaces for fixation by tissue ingrowth. Clin Orthop Relat Res. 1983;176:42–51.
21. Pilliar RM. Porous-surfaced metallic implants for orthopedic applications. J Biomed Mater Res. 1987;A1:1–33.

22. Lampman S. Titanium and its alloys for biomedical implants. In: Narayan R, editor. ASM handbook, Vol 23, materials for medical devices. Materials Park: ASM International; 2012. p. 223–36.
23. Ankem S, Seagle SR. Heat treatment of metastable beta titanium alloys. In: Rosenberg H, Boyer RR, editors. Beta titanium alloys in the 1980's. New York: AIME; 1984. p. 107–26.
24. Long M, Rack HJ. Titanium alloys in total joint replacement – a materials science perspective. Biomaterials. 1998;19:1621–39.
25. Mishnaevsky L Jr, et al. Nanostructured titanium-based materials for medical implants: modeling and development. Mater Sci Eng. 2014;R81:1–19.
26. Yue S, Pilliar RM, Weatherly GC. The fatigue strength of porous-coated Ti-6Al-4V implant alloy. J Biomed Mater Res. 1984;18:1043.
27. Bania PJ. Beta titanium alloys and their role in the titanium industry. In: Eylon D, Boyer RR, Koss DA, editors. Beta titanium alloys in the 1990's. Warrendale: The Minerals, Metals & Materials Society; 1993. p. 3–14.
28. Mishra AK, Davidson JA, Poggie RA, Kovacs P, Fitzgerald TJ. Mechanical and tribological properties and biocompatibility of diffusion hardened Ti-13Nb-13Zr – a new titanium alloy for surgical implants. In: Medical applications of titanium and its alloys: the material and biological issues, ASTM STP1272. West Conshohocken: ASTM International; 1996. p. 96–113.
29. Benezra V, Mangin S, Treska M, Spector M, Hunter G, Hobbs LW. Microstructural investigation of the oxide scale of Zr-2.5Nb and its interface with the alloy substrate, in biomedical materials-drug delivery. Implants and tissue engineering. Mater Res Soc Symp Proc. 1999;550:337–42.
30. Garrett S, Jacobs N, Yates P, Smith A, Wood D. Differences in metal ion release following cobalt-chromium and oxidized zirconium total knee arthroplasty. Acta Orthop Belg. 2010;76(4):513–20.
31. Lewis PM, Moore CA, Olsen M, Schemitsch EH, Waddell JP. Comparison of mid-term clinical outcomes after primary total hip arthroplasty with Oxinium vs cobalt chrome femoral heads. Orthopedics. Dec 2008;31(12 Suppl 2):371–83.
32. Haasters J, v Salis-Salio G, Bensmann G. The use of Ni-Ti as an implant in orthopaedics. In: Deurig TW, Melton KN, Stockel D, Wayman CM, editors. Engineering aspects of shape memory alloys. London: Butterworth-Heinemann; 1990. p. 426–44.
33. Wever DJ, Veldhuizen AG, Sanders MM, Schakenrad JM, van Horn JR. Cytotoxic, allergic and genotoxic activity of a nickel-titanium alloy. Biomaterials. 1997;18:1115–20.
34. Kapanen A, Ryhanen J, Danilov A, Tuukkanen J. Effect of nickel-titanium shape memory alloy on bone formation. Biomaterials. 2001;22:2475–80.
35. Firstov GS, Vitchev RG, Kumar H, Blanpain B, Van Humbeeck J. Surface oxidation of NiTi shape memory alloy. Biomaterials. 2002;23:4863–71.
36. Cisse O, Savadogo O, Wu M, Yahia LH. Effect of surface treatment of NiTi alloy on its corrosion behavior in Hanks' solution. J Biomed Mater Res. 2002;61:339–45.
37. Assad M, Chernyshov AV, Jarzem P, Leroux MA, Coillard C, Charette S, Rivard C-H. Porous titanium-nickel for intervertebral fusion in a sheep model: part 2. Surface analysis and nickel release assessment. J Biomed Mater Res B Appl Biomater. 2003;64B:121–9.
38. Zardiackas LD, Parsell DE, Dillon LD, Mitchell DW, Nunnery LA, Poggie R. Structure, metallurgy and mechanical properties of a porous tantalum foam. J Biomed Mater Res Appl Biomater. 2001;58:180–7.
39. Bobyn JD, Stackpool GJ, Hacking SA, Tanzer M, Krygier JJ. Characteristics of bone ingrowth and interface mechanics of a new porous tantalum biomaterial. J Bone Joint Surg. 1999;81-B:907–14.
40. O'Brien BJ, Stinson JS, Larsen SR, Epihimer MJ, Carroll WM. A platinum-chromium steel for cardiovascular stents. Biomaterials. 2010;31(14):3755–61.
41. Chen Y, Xu Z, Smith C, Sankar J. Recent advances on the development of magnesium alloys for biodegradable implants. Acta Biomater. 2014;10:4561–73.

42. Kusmerczyk K, Basista M. Recent advances on magnesium alloys and magnesium -calcium phosphate composites as biodegradable implant materials. J Biomater Appl. 2017;31(6):878–900.
43. Yoshimoto S, Yamasaki M, Kawamura Y. Microstructural and mechanical properties of extruded Mg-Zn-Y alloys with 14H long period ordered structure. Mater Trans. 2006;47:959–65.
44. Erbel R, et al. Temporary scaffolding of coronary arteries with bioabsorbable magnesium stents: a prospective, non-randomised multicenter trial. Lancet. 2007;369:1869–75.
45. Anusavice KJ. Chapter 17: dental amalgam: structures and properties. In: Phillip's science of dental materials. 10th ed. London: W. B. Saunders; 1996.
46. Poinern GEJ, Brundavanam S, Fawcett D. Biomedical magnesium alloys: a review of material properties, surface modifications and potential as a biodegradable orthopedic implant. Am J Biomed Eng. 2012;2(6):218–40.
47. Mishnaevsky L Jr, et al. Nanostructured titanium-based materials for medical implants: modeling and development. Mater Sci Eng R. 2014;81:1–19.
48. Yang L. Nanotechnology-enhanced metals and alloys for orthopedic implants. In: Nanotechnology-enhanced orthopedic materials, Woodhead Publishing series in biomaterials. Kent: Elsevier; 2015. p. 27–47.
49. Padilla HA II, Boyce BL. A review of fatigue behavior in nanocrystalline metals. Exp Mech. 2010;50(1):5–23.
50. Baker SP. Plastic deformation and strength of materials in small dimensions. Mater Sci Eng. 2001;319–321:16–23.
51. Boyce BL, Padilla HA II. Anomalous fatigue behavior and fatigue-induced grain growth in nanocrystalline nickel alloys. Metall Mater Trans A. 2011;42A:1793.
52. Cheng D, Tellkamp VL, Lavernia CJ, Lavernia EJ. Cprrosion properties of nanocrystalline Co-Cr coatings. Ann Biomed Eng. 2001;29:803–9.
53. Edwards P, Ramulu M. Fatigue performance evaluation of selective laser meltedTi-6Al-4V. Mater Sci Eng A. 2014;598:327–37.